TRAJECTORY OPTIMIZATION FOR CELLULAR-CONNECTED UAV IN FUTURE WIRELESS NETWORKS

DU XIANGMING

MPhil

The Hong Kong Polytechnic University

2025

The Hong Kong Polytechnic University

Department of Electrical and Electronic Engineering

Trajectory Optimization for Cellular-Connected UAV in Future Wireless Networks

DU Xiangming

A thesis submitted in partial fulfilment of the requirements for the degree of Master of Philosophy

August 2024

CERTIFICATE OF ORIGINALITY

I hereby declare that this thesis is my own work and that, to the best of my knowledge and belief, it reproduces no material previously published or written, nor material that has been accepted for the award of any other degree or diploma, except where due acknowledgement has been made in the text.

_____

DU Xiangming

7 March 2025

Abstract

Cellular-enabled unmanned aerial vehicle (UAV) communication or cellular-connected UAV is a promising approach for realizing high-quality UAV-to-ground communications. In this thesis, we investigate brand new challenges for cellular-connected UAVs, separately focusing on a sensing problem for a target whose exact location is unknown and random and a handover awareness problem for cellular-enabled UAV communication.

Firstly, we study a trajectory optimization of a cellular-connected UAV which bears a mission of sensing the location of a ground target based on its prior location distribution information where the UAV maintains satisfactory communication with ground base stations (GBSs). We focus on a challenging scenario where the exact location of the target to be sensed is unknown and random, while its prior distribution is known and stored in a novel target location distribution map. Based on this map, the probability for the UAV to successfully sense the target can be extracted as a function of the UAV's location. The UAV exploits the target location distribution map to visit specific locations to maximize the sensing probability. We aim to optimize the UAV's trajectory between two pre-determined locations to maximize the total sensing probability during its flight, subject to a GBS-UAV communication quality constraint at each time instant during its flight and a maximum mission completion time constraint. However, this new problem is a constrained longest path problem (CLPP), which is non-convex and NP-Hard. Particularly, the optimal trajectory

needs to strike the best balance between the total probability, expected SNR, and maximum flying distance. To address this problem, we propose three high-quality suboptimal solutions, which can achieve significantly improved sensing performance.

Secondly, we study a cellular-connected UAV which aims to complete a mission of flying between two pre-determined locations while maintaining satisfactory communication quality with the GBSs. Due to the potentially long distance of the UAV's flight, frequent handovers may be incurred among different GBSs, which leads to various practical issues such as large delay and synchronization overhead. To this end, we mathematically derive the handover function, which is critically dependent on the UAV's trajectory and GBS-UAV associations. We aim to minimize the number of GBS handovers by jointly optimizing the UAV's flight trajectory and the GBS-UAV association, subject to a communication quality constraint and a maximum mission completion time constraint. Although this problem is non-convex and difficult to solve, we derive useful structures of the optimal solution, based on which we propose an efficient algorithm based on graph theory and Lagrangian relaxation for finding a high-quality suboptimal solution in polynomial time. Numerical results validate the effectiveness of our proposed trajectory design.

In summary, this thesis studies two cellular-connected UAV trajectory optimization problems in future wireless networks, and proposes high-quality solutions to tackle them. For sensing a target without exact location information, the proposed trajectory designs achieve significantly improved sensing performance by leveraging the prior location distribution information of the target, which provides a useful guideline for cellular-connected UAVs to sense targets. Moreover, the investigation of handovers provides a new model for handover analysis, and the designed trajectory significantly decreases the number of handovers, which provides valuable principles for cellular-connected UAVs on their

safe flight.

Publications

- **X. Du**, S. Zhang, and L. Liu, "UAV trajectory optimization for sensing exploiting target location distribution map," in *Proc IEEE Vehicular Technology Conference (VTC) Spring*, Jun. 2024.

- **X. Du**, S. Zhang, and F. C. M. Lau, "Handover-aware trajectory optimization for cellular-connected UAV," accepted to appear in *IEEE Wireless Communications Letters*.

Acknowledgements

Firstly, I would like to express my deepest gratitude to my supervisors, Prof. Shuowen Zhang and Prof. Francis C.-M. Lau, for their care, guidance, and encouragement throughout my master's study. My chief supervisor, Prof. Shuowen Zhang, not only provided me with academic guidance, but also gave me a lot of valuable advice on my life. I want to express my deepest thanks to her for always guiding me patiently and helping me. I am forever grateful for the countless hours she spent revising drafts, discussing ideas, and encouraging me to push the boundaries of my understanding. My co-supervisor, Prof. Francis C.-M. Lau, provided me with a lot of insightful guidance and constant encouragement. His critical comments, rich experience, and valuable advice have shaped not just this thesis, but also my growth. I feel very lucky to have the opportunity to receive their academic guidance.

I am also deeply thankful for the support of my colleagues and friends, especially the members of Prof. Zhang's group. Your companionship, encouragement, and suggestions have made these two years the most memorable in my life. Our shared experiences, late-night discussions, and support of being there for each other have been a source of strength that I will always cherish.

Finally, I dedicate all my love and gratitude to the two most important people in my life, my dear parents. Without your love, I would not have been able to get to this point. I hope my father and mother are well.

Contents

List of Figures

List of Symbols

Throughout this thesis, scalars are denoted by lower-case letters, vectors are denoted by bold-face lower-case letters, and matrices are denoted by bold-face upper-case letters. In addition, we define the following symbols:

$\|\boldsymbol{x}\|$	the Euclidean norm of a vector $\boldsymbol{x}$
$\dot{\boldsymbol{x}}(t)$	the first-order derivative of $\boldsymbol{x}$ with respect to time t
$\boldsymbol{X}^T$	the transpose of a matrix $\boldsymbol{X}$
$[\boldsymbol{X}]_{i,j}$	the (i,j)-th element of a matrix $\boldsymbol{X}$
$\|\mathcal{X}\|$	the cardinality of a set $\mathcal{X}$
$\mathcal{X}\backslash\mathcal{Y}$	the set $x \| x \in \mathcal{X}$ and $x \notin \mathcal{Y}$
$\mathbb{E}[\cdot]$	the statistical expectation
$\mathcal{O}(\cdot)$	the standard big-O notation
$\mathbb{R}^{m\times n}$	the space of $m \times n$ real matrices
$\mathbb{C}$	the space of complex numbers
$\triangleq$	"defined as"

1. Introduction

Unmanned Aerial Vehicles (UAVs), commonly known as drones, have seen rapid advancements and widespread applications across various sectors. Specifically, UAVs are employed in various missions in both areas of human activity and natural environments, depending on their strong maneuverability under three-dimensional (3D) [1–6]. For instance, in environmental protection, UAVs can detect gas/oil spills and assist in litter collection [7–9]; in the military, UAVs provide reconnaissance, surveillance, and combat support [10, 11]; in agriculture, UAVs are used for pesticide spraying and vegetation monitoring [12, 13]; UAVs have become invaluable in rescue operations by providing communication services and delivering supplies [14, 15]. To fully exploit and enhance the application value of UAVs, numerous practical problems have been identified and comprehensively researched, e.g., UAV trajectory design, UAV swarming design, and UAV deployment. However, with the innovation of wireless communication technologies, massive missions that UAVs can achieve are rising, thereby deriving further investigation into UAV application problems.

To achieve various flight missions, it is of paramount importance to ensure that UAVs can be timely operated, which requires high-quality communications between UAVs and their controllers. To ensure the safety of UAVs, an efficient solution is *cellular-enabled UAV communication* or *cellular-connected UAV*, where UAVs act as a new type of aerial users served by the ground base stations (GBSs) in the cellular network [15–23]. Specifically, by utilizing GBSs to serve

UAVs in cellular networks, the links between the UAVs and GBSs can achieve ultra-reliable, low latency, and high-speed backhaul links, which effectively supports low-rate two-way control and non-payload communication (CNPC) for ensuring the safety of UAVs and the high-rate payload communication (PC) for the deliveration of acquire information to the cellular network. Compared with traditional Wi-Fi based UAV communication, cellular-enabled UAV communication can extend the service range from visual line-of-sight (VLoS) to beyond VLoS, thus supporting much longer flying distances and much wider application scenarios. The exploration of cellular-connected UAVs promises numerous applications, such as enhanced delivery services, improved disaster response, and efficient traffic monitoring and management. However, this integration between cellular networks and UAVs introduces challenges, particularly in terms of network congestion, interference management, and ensuring reliable and secure communication links. It is worth noting that although many existing works have studied these challenges, e.g., [15–17, 19, 20], with the development of wireless networks in the future, the upgrade of wireless network technology will not only make such challenges more complicated, but also generate more new challenges.

To overcome those challenges for cellular-connected UAVs in future wireless networks, one of the keys to cellular-connected UAVs in practical applications is trajectory optimization or so-called path planning. Specifically, by exploiting the cellular-connected UAV's flexibility in 3D space, flight mission requirements and enhanced performance can be achieved via the proper design of the UAV's trajectory. To this end, the cellular-connected UAV trajectory design aims to optimize the flight trajectory for UAVs to achieve specific objectives while adhering to various constraints. In detail, the objectives and constraints of cellular-connected UAV trajectory optimization are mainly based on the consideration of personalized missions and UAV flight safety, among which representative ones include minimizing flight time, minimizing energy consumption, and avoiding

obstacles [17, 19, 24–32]. In addition, it is worth noting that how to effectively improve the communication performance of cellular-connected UAVs by designing their trajectories is also a challenging problem, such as sum-rate maximization, throughput maximization, and interference minimization [19,20,25,33]. On the other hand, the evolving UAV products have richer and more diverse functions, and the development of wireless network technology has brought more in-depth mission requirements, both of which have caused the application scenarios of UAVs to increase dramatically, but the UAV trajectory optimization problem has also become more challenging simultaneously, e.g., applications for integrated sensing and communication (ISAC), terahertz (THz) spectrum, and intelligent reflecting surfaces assisted UAV. In order to further expand the space for cellular-connected UAV applications, this thesis is dedicated to solving brand new challenging trajectory optimization problems for cellular-connected UAVs in practice.

The rest of this chapter is organized as follows. Section 1.1 presents an overview of UAV trajectory optimization. Section 1.2 provides the motivations and challenges of the problems proposed in this thesis. Section 1.3 and Section 1.4 present the organization and major contributions of this thesis, respectively.

1.1. Overview of UAV Trajectory Optimization

In this section, we provide an overview of UAV trajectory optimization. Specifically, we first introduce the basic concept of UAV and specify several typical trajectory designs. Then, we highlight challenges for UAV trajectory optimization in wireless networks. Finally, we propose some future applications that UAV trajectory optimization can achieve.

1.1.1 Introduction to UAV Trajectory Optimization

UAV trajectory optimization is a vital area of research and development aimed at enhancing the performance and efficiency of UAV operations. By determining optimal flight paths, UAVs can ensure efficient energy usage, maintain robust connectivity with cellular networks, and adapt to dynamic environments. This optimization process is essential for maximizing the UAVs' capabilities and integrating them into future wireless networks. The trajectory optimization of UAVs mainly aims to ensure the safety of UAVs and complete given missions [15, 17, 19, 34–41]. Specifically, a UAV bears some missions while maintaining satisfactory communication quality with one of M GBSs. The UAV needs to fly to complete these missions, where the time-varying location of the UAV is given by $\boldsymbol{u}(t) = (x(t), y(t), H(t)),\ 0 \le t \le T$, as shown in Fig. 1.1. By optimizing flight trajectory $\{\boldsymbol{u}(t),\ 0 \le t \le T\}$, the UAV can safely fly along the designed trajectory with the consideration of speed V meters/second (m/s), height $H(t)$, mission requirements, etc.

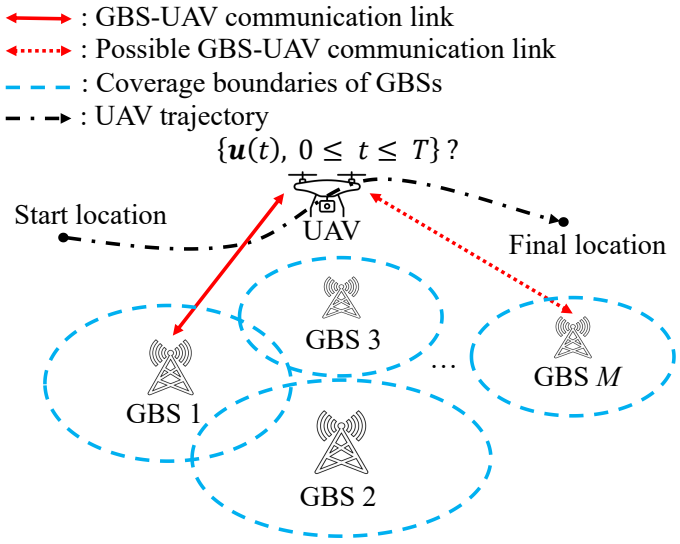

Figure 1.1: Illustration of trajectory design for a UAV with considerations of missions and communication.

It is worth noting that the UAV can be employed in more complex missions that are derived from the development of wireless network technology. [15, 17, 19]

studied the cellular-connected UAV trajectory optimization for communication performance improvement, including the outage duration, interference management, and connectivity. The promising ISAC technology involves UAVs performing sensing tasks while maintaining communication links. This dual functionality is essential for applications such as environmental monitoring and smart city infrastructure. For instance, [33, 42–44] achieved better sensing performance by optimizing the UAV trajectory with the joint consideration of advanced beamforming techniques. Tracking applications require UAVs to follow or maintain a line of sight with a moving target. This is crucial in scenarios like wildlife monitoring, law enforcement, and search and rescue operations. [45–47] investigated the UAV trajectory optimization problem for tracking, which involves following a moving target to gather data or maintain surveillance.

1.1.2 Challenges of UAV Trajectory Optimization

UAVs have inherent advantages of low cost, flexible deployment, and high maneuverability, which make them well suited to perform a variety of missions that are challenging or impractical for ground systems. By optimizing their trajectories, UAVs can maximize these advantages, ensuring that they operate efficiently in various scenarios. However, optimizing trajectories of UAVs for various missions generally involves addressing several complex constraints and challenges:

Connectivity: Ensuring uninterrupted connectivity with the cellular network is crucial for real-time data transmission and control. UAVs must navigate areas with varying signal strengths and avoid dead regions where connectivity is lost, in which the UAV trajectory optimization should consider the locations of GBSs.

Energy Efficient and Power: UAVs are typically powered by batteries, which have limited capacity. Efficient energy management is essential to

extend flight time and operational range. Trajectory optimization should consider energy consumption to ensure UAVs can complete their missions without exhausting their power supply.

Collision Avoidance: UAVs often operate in environments with various obstacles, such as buildings, trees, and other structures. Obstacle detection and avoidance are necessary to prevent collisions and ensure safe operation for UAV flights. In particular, urban environments with their dense and varied structures, present more challenges for trajectory optimization, as UAVs must fly through tight spaces. Moreover, the trajectory optimization for a UAV swarm must consider the collision problem with other UAVs.

Communication Constraints: UAV trajectory optimization should achieve various communication constraints, such as signal strengths and SNR constraints, which ensures the UAV can successfully receive the control command. Meanwhile, there are other considerations in some special scenarios, e.g., the rate for data transmission, the secret rate for UAV communication against eavesdroppers, interference, and spectrum management.

Regulatory and Safety Constraints: UAV operations are subject to a range of regulatory constraints, including restrictions on flight paths, altitude limits, and no-fly zones. Additionally, UAVs must be operated in a manner that ensures safety for people and property on the ground. Moreover, UAVs must adhere to local, national, and international regulations, which can vary widely depending on the location and type of operation. Compliance with these regulations is essential to ensure safe and legal operation.

Handling Environmental Factors: Environmental conditions, such as wind, rain, and temperature, can significantly affect UAV performance. Trajectory optimization should account for these factors to ensure that UAVs can complete their mission safely and effectively.

Nevertheless, other important challenges in UAV trajectory optimization

come from mission objectives. In general, the coupling between customized mission objectives and the challenges mentioned above makes the trajectory optimization problem more difficult to solve. To address these challenges, tailored trajectory optimization algorithms should be developed that enable UAVs to perform their missions effectively while maintaining reliable connectivity and adhering to regulatory requirements.

1.1.3 Future Applications of UAV Trajectory Optimization

UAV trajectory optimization added to future wireless networks (e.g., 6G and beyond) opens up a wide range of advanced applications in various fields. The integration of UAVs with future wireless networks will enable UAVs to perform missions more efficiently, reliably, and intelligently. The following are some key future applications that UAV trajectory optimization can achieve:

Autonomous Air to Ground Traffic Command: In the future, using UAVs to control ground traffic is a viable solution, especially for dealing with road congestion. By optimizing UAVs' trajectories, UAVs can safely and quickly fly to congested sections in crowded urban environments, and use sensing and data analysis technologies to analyze the causes of road congestion and quickly solve it. In addition, future wireless networks can support ultra-low latency communications, allowing real-time adjustments to UAV trajectory designs based on changing traffic patterns, weather conditions, and other variables, which ensures the safety and operational efficiency of UAV command systems.

Disaster Response and Emergency Services: UAVs can be deployed rapidly in disaster areas to assess damage, support service, and deliver essential supplies. Trajectory optimization allows UAVs to navigate complex environments, avoid hazards, and prioritize critical areas for inspection or delivery. Advanced wireless networks can provide a strong communication link, enabling

UAVs and ground teams to coordinate in real time. Meanwhile, UAVs can also assist future wireless networks in providing communication services and completing missions such as target sensing and survivor localization.

Precision Agriculture: UAVs will be able to effectively monitor large areas of farmland to ensure that crops receive the appropriate amount of water and nutrients and are protected from pests. The UAV trajectory design allows UAVs to cover the field in the most effective mode, reducing overlap and ensuring complete coverage. Future wireless networks will provide real-time data connectivity, allowing UAVs to adjust their paths based on sensing data, weather conditions, and crop health indicators, which can significantly improve agricultural productivity and resource efficiency.

Smart Infrastructure Management: UAVs will be deployed to inspect and monitor infrastructure such as bridges, power lines, and pipelines. Optimized UAV trajectories will enable UAVs to effectively cover large infrastructure networks, ensuring thorough inspections while minimizing flight time and energy consumption. Future wireless networks will support high-bandwidth data transmission, enabling UAVs to send real-time video and sensing data back to control centers for immediate analysis, which will enhance the ability to detect and respond to potential problems in critical infrastructure.

Privacy and Security in ISAC Systems: While ISAC offers significant benefits, such as spectrum efficiency and reduced hardware costs, it also raises new challenges, particularly concerning the privacy and security of non-sensing targets. These non-sensing targets in ISAC systems should be protected, ensuring that their information is not inadvertently disclosed or abused. One promising solution involves exploiting UAVs to enhance privacy and security within ISAC systems. UAVs can be deployed to actively protect non-sensing targets by introducing artificial noise, creating physical barriers, or performing other privacy-preserving actions, which can be achieved by utilizing advanced

point-to-point communication in future wireless networks.

1.2. Motivations and Challenges

In this section, we specify two key challenges for the trajectory optimization of cellular-connected UAVs, which are not yet addressed in the existing literature, thus motivating our investigation in this thesis.

1.2.1 How to Sense a Target Whose Location Is Random and Unknown for Cellular-Connected UAV?

Motivated by the emergence of new applications which require the *sensing* function, the role of UAV in performing sensing missions has recently attracted significant research attention [33, 48–52]. Specifically, by exploiting the UAV's flexibility in the three-dimensional (3D) space, enhanced sensing performance can be achieved via the proper design of the UAV's trajectory. However, existing studies typically considered the ideal scenario where the exact locations of the targets to be sensed are *known*. Based on the known exact locations of targets, many traditional sensing missions can be addressed, mainly including localization, data acquisition, speed estimation, etc. For instance, [20] considered the case where multiple known target locations need to be visited for sensing; [43, 53] aimed to ensure that sufficient power is radiated to every target location; [54] studied the achievable rate maximization problem with the consideration of given target locations and user locations; [55] proposed a trade-off between the time for UAV sensing and that for UAV transmission during UAV sensing target.

However, in practice, such exact location information may not be available. Moreover, the target may appear at different locations with distinct probabilities, which cannot be characterized by existing models and studies. In this

thesis, we consider a practical and challenging scenario where the exact target location is *unknown* and *random*, while its statistical distribution is known *a priori* based on empirical measurements or target movement pattern [56–59]. It is worth noting that the scenario we consider is a reflection of many real application problems, especially in the field of environmental protection. One such application is detecting and modeling oil spill regions, a critical mission requiring precise and timely intervention to mitigate environmental damage. In practice, since the oil spills are dynamic and prone to drifting due to currents and winds, the possible spill regions are unknown and random. We leverage UAVs to sense oil spill regions for collecting data. The obtained data can be used to analyze and model oil spill regions, providing an innovative and efficient solution for this environmental pollution event. By designing UAV flight trajectories, UAVs can maximally sense potential spill regions. In detail, the UAV needs to conduct control communication with the GBSs, and simultaneously send sensing signals to obtain the oil layer information. The other application is UAV-assisted forest health assessment, which aims to leverage UAVs to monitor and evaluate large forested areas efficiently and accurately. When any anomalies are presented in the obtained images as the prior information, we need to further sense the locations where anomalies may appear. Since the spread of anomalies in the forest is unknown and random, we can obtain the statistical characteristics of the locations where anomalies appear based on some empirical measurements or propagation patterns. This knowledge allows us to optimize UAV flight trajectories to ensure that high-risk areas are inspected more frequently and thoroughly. These scenarios can be represented by a simple model, as shown in Fig. 1.2.

we propose a novel *target location distribution map* to characterize and store the probabilities of the appearance of the target over a geographical region, which can also quantify the probabilities for the UAV to successfully sense the target when it flies to the waypoint near each possible location. Based on this, how to

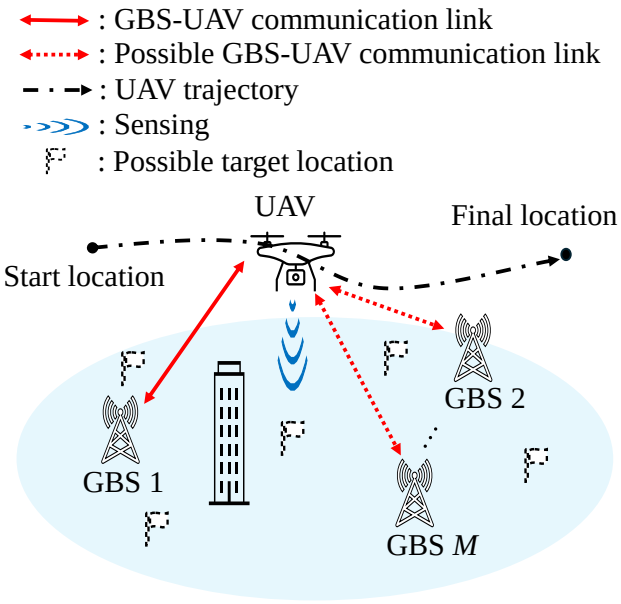

Figure 1.2: Illustration of a target sensing model for a cellular-connected UAV.

design the UAV's trajectory for maximizing the overall probability of successfully sensing a target during its flight is a new challenging problem, which requires careful exploitation of the target location distribution map such that the UAV can prioritize its flight near highly-probable target locations. Moreover, how to guarantee satisfactory communication quality with the GBSs while performing the UAV's sensing task efficiently is also an open problem, which requires the trajectory design to strike the optimal balance among communication, sensing, and mission completion performances.

Motivated by the above communications and sensing issues, we aim to devise the trajectory optimization of a cellular-connected UAV that can achieve the best balance between the sensing mission, satisfactory communication performance, and the constraints for flight requirements.

1.2.2 How Will Network Handovers Affect the Flight Trajectory for Cellular-Connected UAV?

To maintain satisfactory communication quality with the GBSs, the UAV's trajectory needs to be carefully designed. Particularly, there exists a non-trivial trade-off between the communication quality and the mission completion performance (e.g., mission completion time), since the UAV should generally fly near the GBSs to enhance the communication link quality, which, on the other hand, may result in detoured paths in completing the mission. [15] studied the trajectory optimization for minimizing the mission completion time subject to a constant communication quality constraint throughout the flight, and proposed an efficient polynomial-time algorithm for finding an approximate solution with arbitrarily low performance gap with the optimal solution. [17] extended this work by allowing tolerable connection disruptions with the GBSs, while [19, 60] took the interference issue into consideration. On the other hand, [20] studied the communication-constrained UAV trajectory design for the specific mission of information collection.

However, a critical practical issue overlooked in the existing literature lies in the potentially frequent *handovers* among multiple GBSs that consecutively associate with the UAV. Specifically, to complete a given flight mission, UAVs will fly long distances in the cellular network in general. If UAVs must fly to a waypoint that exceeds the coverage boundary of a single GBS in the cellular network, the network handover is inevitable for the completion of the given mission, as shown in Fig. 1.3. Due to the generally long distances of the UAV's flight, the UAV may have to frequently change the associated GBS, which may cause heavy signaling overhead and affect the service continuity [61–63]. Specifically, network handovers involve multiple signaling exchanges between the UAV, the current GBSs, and the next GBSs, which include steps such as measuring signal quality,

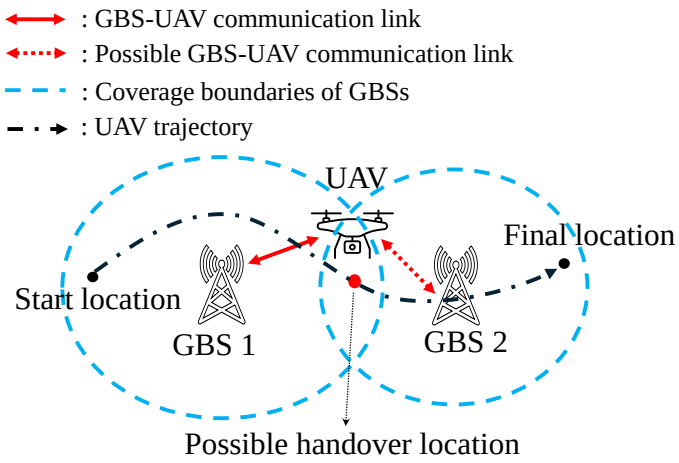

Figure 1.3: Illustration of an inevitable handover in cellular-connected UAV trajectory design.

making the handover decision, disconnecting the connection, and establishing a new connection. Many works focus on reducing network handovers to achieve seamless communication, but there is always a risk of temporary service disruption during the handover from one GBS to another GBS. For instance, in hard handovers (break-before-make), UAVs momentarily disconnect from the current GBS before establishing a connection with the next one, leading to brief interruptions in communication [64]. For soft handovers (make-before-break), where the UAV connects to the new GBS before disconnecting from the current one, there can still be issues related to synchronization and data consistency [65, 66]. These disruptions can be particularly problematic in applications, such as real-time video streaming, remote control of UAVs, or emergency response operations, since even a brief communication loss may lead to operational failures. In addition, the ping-pong effect caused by frequent handovers will downgrade the network security [67–69]. Experiments have shown that increasing the number of handovers leads to more frequent delay peaks [70, 71]. Although the handover issue has been analyzed and studied in e.g., [61, 63, 72–75], how to minimize the number of handovers via UAV trajectory design is still an unaddressed open problem, which motivates the study in this thesis.

Motivated by this, we aim to formulate the total number of handovers and

study the trajectory optimization problem for a cellular-connected UAV, which can minimize the total number of handovers during the UAV flight.

1.3. Organization of the Thesis

Motivated by the above challenging issues, in this thesis, we study the cellular-connected UAV trajectory optimization under the following two scenarios: a cellular-connected UAV bears a sensing mission, which requires the UAV to fly to sense a target whose location is random and unknown within a given maximum flight distance constraint; moreover, a new cellular-connected UAV has a mission to fly from an initial location to a final location, where we aim to minimize the number of handovers to avoid the degrade of quality of service. The rest of this thesis is organized as follows.

In Chapter 2, we propose a target location distribution map to characterize the target location information and the sensing performance to overcome the challenges of the sensing mission. We study the sensing performance maximization problems by optimizing the trajectory of the cellular-connected UAV. The proposed solutions can significantly increase their performance compared with benchmarks.

In Chapter 3, to solve the handover minimization problem, we model a novel handover function to represent the number of handovers during the UAV flight. We study a trajectory optimization problem for the cellular-connected UAV, which is NP-Hard and non-convex. To address this challenging issue, we propose a high-quality approximation solution based on some structural properties. Numerical results validate that the number of handovers in our proposed design is significantly decreased and outperforms the benchmark scheme.

In Chapter 4, we conclude this thesis and propose some useful guidelines for future work.

1.4. Major Contributions

The major contributions of this thesis are summarized as follows.

1.4.1 Useful Guidelines of Trajectory Optimization of Cellular-connected UAVs for Sensing

In Chapter 2, we draw useful guidelines for the cellular-connected UAV trajectory design for target sensing. The detailed contributions of this chapter are summarized as follows:

- First, we propose a *target location distribution map* to characterize and store the probabilities of the appearance of the target over a geographical region. Leveraging the target information presented by *target location distribution map*, we can quantify the probabilities for the UAV to successfully sense the target when it flies to the waypoint near each possible location under 3D space. By utilizing this map, the objective function is derived as the total sensing probability, and based on this, our goal is to maximize this objective function by optimizing the UAV trajectory.

- Next, we study the trajectory optimization of a cellular-connected UAV which bears a mission of sensing the location of a ground target based on its prior location distribution information, while maintaining satisfactory communication quality with the GBSs for ensuring its safety. We consider a general channel with potential obstructions between the UAV and GBSs, and propose to adopt the *radio map* technique for characterizing the expected signal-to-noise ratio (SNR) at each UAV's possible location [19, 76–78]. We aim to optimize the UAV's trajectory to maximize the *total (overall) probability* for successfully sensing the target, subject to a minimum expected SNR threshold at each time instant during

the UAV's flight and a mission completion time constraint. This problem is non-convex and NP-hard. In particular, our object is completely opposite to the traditional objects in the UAV trajectory optimization problems that minimize the flight time or distance during the UAV flight (e.g., [15, 17, 20, 43, 49, 51]), which is of high practical and novel interest in UAV trajectory optimization.

- Finally, by exploiting the unique structures of the problem, we propose three algorithms for finding high-quality suboptimal solutions with polynomial complexity. Based on our proposed solutions, the total sensing probability is significantly improved for the different parameters of maximum mission completion time. Numerical results show that our proposed designs achieve significantly increased total sensing probability compared to the conventional shortest-distance trajectory design.

To the best of our knowledge, this work is the first to consider using the prior probability distribution information of the target location to design the constrained longest path when the UAV flies to sense the target. To overcome the challenges posed by the nature that the target location is random and unknown, we consider a promising model that cellular-enabled UAV communication supports the UAV in sensing more possible target locations safely. As a new work focused on prolonging trajectory to improve sensing performance, we consider offline trajectory optimization for sensing the target under the communication constraint, thus being a valuable framework for the case that path design requires passing through more inspection points in practice.

1.4.2 Efficient Handover-aware Trajectory design for Cellular-Connected UAV

In Chapter 3, we draw useful guidelines for the cellular-connected UAV trajectory design for handover minimization. The detailed contributions of this chapter are summarized as follows:

- First, we mathematically define a novel *handover function* to represent the number of handovers by characterizing the connection and disconnection behaviors for GBS-UAV communication while the UAV flies at the cellular network. By utilizing the *handover function*, the objective function is derived as a step function, and based on this, our goal is to minimize this objective function by optimizing the UAV trajectory.

- Next, we consider a cellular-connected UAV which needs to fly from a given initial location to a given final location. To ensure its safety, it needs to maintain a satisfactory communication quality constraint with a GBS at every time instant. We aim to optimize the UAV's trajectory to minimize the number of handovers during the flight, subject to the communication quality constraint and a maximum threshold on the mission completion time. This problem is non-convex and difficult to solve.

- By judiciously exploring the problem structure, we transform the problem into a more tractable form, based on which we propose a polynomial-time algorithm by applying graph theory and Lagrangian relaxation to find a high-quality suboptimal solution. It is shown via numerical results that our proposed design requires fewer handovers compared with handover-unaware trajectory design.

To our understanding, this work is the first to consider network handovers for designing the UAV trajectory. We propose a novel mathematical model

that characterizes the connection and disconnection processes in GBS-UAV communications, enabling the calculation of the total number of handovers. This work focused on the affection of network handovers for trajectory design of the cellular-connected UAV, and we consider offline trajectory optimization that aims to minimize the total number of handovers under the connectivity constraint. Moreover, this work provides valuable insights into the selection of communication performance metrics, particularly in scenarios where users or ground vehicles require high-quality communication services in practice.

2. UAV Trajectory Optimization for Sensing Exploiting Target Location Distribution Map

2.1. Introduction

In this chapter, we study the trajectory optimization of a cellular-connected UAV which aims to sense the location of a target while maintaining satisfactory communication quality with the GBSs. In contrast to most existing works which assumed the target's location is known [43, 53], we focus on a more challenging scenario where the exact location of the target to be sensed is *unknown* and *random*, while its distribution is known *a priori* and stored in a novel *target location distribution map*. Based on this map, the probability for the UAV to successfully sense the target can be extracted as a function of the UAV's trajectory. On the other hand, to achieve satisfactory communication between GBSs and the UAV, the channel characteristics are presented by utilizing the *radio map* technique. We aim to optimize the UAV's trajectory between two pre-determined locations to maximize the *overall sensing probability* during its flight, subject to a GBS-UAV communication quality constraint at each time instant and a maximum mission completion time constraint. Despite the non-convexity and NP-hardness of this problem, we devise three high-quality suboptimal solutions

tailored for it with polynomial complexity. Numerical results show that our proposed designs outperform various benchmark schemes.

The remainder of this chapter is organized as follows. Section 2.2 presents a literature review. Section 2.3 introduces the system model, including the communication model and the target sensing model. Section 2.4 presents the trajectory optimization problem. Section 2.5 reformulates a more tractable problem and further presents three efficient and alternative approaches to the initial problem. Numerical results are provided in Section 2.6 to evaluate the performance of proposed solutions. Finally, Section 2.7 concludes the chapter.

2.2. Literature Review

UAVs combined with sensing technologies have become a crucial approach across various fields, including agriculture, environmental monitoring, and disaster management. This section highlights key research studies that have explored different aspects of UAV-based sensing technologies, discussing their contributions, methodologies, and findings.

UAV-enabled sensing has been studied in many works. UAVs can carry a hardware device to sense a target, e.g., high-resolution optical cameras and radars. [51] studied radar sensing for cellular-connected UAVs, where the UAV's trajectory in terms of energy efficiency is designed. [45] considered that ground targets with radio transmitters can send radio signals that can be captured by the UAV for tracking. Furthermore, ISAC is a promising new sensing technology that integrates sensing and communication into a system, enabling UAVs to simultaneously sense targets and transmit data. [33, 48] investigated the use of UAVs on ISAC technology for target sensing. They provided overviews of UAV-enabled ISAC systems and proposed various solutions for sensing performance and communication performance. [43, 44] explored UAV maneuver (deployment

location or flight trajectory) and the transmit beamforming for a UAV-enabled ISAC system, to maximize the communication performance of ground users. They achieved the balances between sensing and communication according to different beampattern gain thresholds. [79] studied a new integrated periodic sensing and communication mechanism for a UAV-enable ISAC system. [50] explored trajectory planning for a cellular-connected UAV to enable an ISAC system.

Note that these works considered that the locations of targets sensed by UAVs are known, or the locations of the sensing areas are determined. However, in practice, the locations of targets may be random and unknown. Therefore, in this case, how to design the UAV trajectory to sense targets has not been studied in the existing works to our best knowledge.

2.3. System Model

We consider a cellular-connected UAV which bears a mission of sensing a target while flying from an initial location U_{S} to a final location U_{F}. Under a 3D Cartesian coordinate system, let $(x_{\mathrm{S}}, y_{\mathrm{S}}, H)$ and $(x_{\mathrm{F}}, y_{\mathrm{F}}, H)$ in meters (m) denote the location coordinates of U_{S} and U_{F}, respectively. To ensure the safety of the UAV, the UAV needs to maintain satisfactory connectivity with the ground via communicating with a GBS in the cellular network. Let $M \geq 1$ denote the number of GBSs that are available for communication. For the purpose of drawing essential insights, we assume that the UAV flies at a constant altitude of H m with constant speed V meters/second (m/s), and let $\mathcal{U} \subset \mathbb{R}^{2\times 1}$ denote the feasible region of the UAV's flight projected to the horizontal plane. Let $\boldsymbol{u}(t) = [x(t), y(t)]^T \in \mathcal{U}$ denote the UAV's horizontal location at each time instant t, and T denote the UAV's mission completion time. We aim to optimize the UAV's horizontal trajectory $\{\boldsymbol{u}(t), 0 \leq t \leq T\}$ to maximize the sensing

performance, subject to a communication quality constraint at each time instant during the flight, and a maximum mission completion time threshold denoted by $\bar{T}$ s which is equivalent to a maximum flying distance threshold given by $\bar{D} = V\bar{T}$ m.

2.3.1 GBS-UAV Communication Model

At every time instant during the UAV's flight, the UAV needs to conduct control and non-payload communication with one of the GBSs for ensuring its safety [15], which requires low data volume and high reliability, thus single-stream transmission is preferred regardless of the numbers of antennas at the GBS and the UAV. In this thesis, we focus on downlink communication from the GBS to the UAV, while our results are also directly applicable to the case of uplink communication. Denote the effective channel gain from the m-th GBS to the UAV at horizontal location $\boldsymbol{u}$ as $g_m(\boldsymbol{u}) = \bar{g}_m(\boldsymbol{u})\tilde{g}_m(\boldsymbol{u}) \in \mathbb{R}$, where $\bar{g}_m(\boldsymbol{u}) \in \mathbb{R}$ and $\tilde{g}_m(\boldsymbol{u}) \in \mathbb{R}$ denote the large-scale channel gain and the small-scale fading gain, respectively, with $\mathbb{E}[\tilde{g}_m^2(\boldsymbol{u})] = 1$. Specifically, $\bar{g}_m(\boldsymbol{u})$ consists of the path loss, shadowing, and antenna gains at the GBS and the UAV, thus being a static function of the location of the m-th GBS, $\boldsymbol{u}$, and the UAV's altitude H. Therefore, $\bar{g}_m(\boldsymbol{u})$ for any $\boldsymbol{u} \in \mathcal{U}$ can be measured or calculated prior to the UAV's flight [19]. On the other hand, $\tilde{g}_m(\boldsymbol{u})$ is determined by the real-time small-scale fading which changes rapidly over channel coherence intervals. Denote P_m as the transmit power at the m-th GBS, and σ^2 as the effective noise power at the UAV receiver. The received SNR at the UAV if the m-th GBS is selected for transmission is given by $\rho_m(\boldsymbol{u}) = \frac{P_m g_m^2(\boldsymbol{u})}{\sigma^2} = \frac{P_m \bar{g}_m^2(\boldsymbol{u})\tilde{g}_m^2(\boldsymbol{u})}{\sigma^2}$.

Since the small-scale fading gain $\tilde{g}_m(\boldsymbol{u})$ is generally a random variable and cannot be known prior to the UAV's flight, we adopt the *expected SNR* as the communication performance metric in the trajectory optimization, and

consider a minimum threshold for it denoted by $\bar{\rho}$.[1] Under this metric, the GBS with the highest expected SNR should be associated with the UAV for communication, which leads to a resulting expected SNR at the UAV given by $\bar{\rho}(\boldsymbol{u}) = \max_{m\in\mathcal{M}} \mathbb{E}[\rho_m(\boldsymbol{u})] = \max_{m\in\mathcal{M}} \frac{P_m \bar{g}_m^2(\boldsymbol{u})}{\sigma^2} \geq \bar{\rho},\ \forall \boldsymbol{u} = \boldsymbol{u}(t),\ 0 \leq t \leq T.$

Note that the expected SNR $\bar{\rho}(\boldsymbol{u})$ is determined by $\bar{g}_m(\boldsymbol{u})$, which consists of the shadowing effect and is critically dependent on the terrain features (e.g., location, height, and shape of the obstacles). In general, it is difficult to analytically model $\bar{g}_m(\boldsymbol{u})$ and consequently $\rho(\boldsymbol{u})$ as explicit and tractable functions of $\boldsymbol{u}$ to facilitate trajectory optimization. In this thesis, we adopt a *map-based approach* to characterize the expected SNR, where the values of $\bar{\rho}(\boldsymbol{u})$ for all $\boldsymbol{u} \in \mathcal{U}$'s are stored in an *expected SNR map* [19]. Specifically, we first quantize the continuous region $\mathcal{U}$ into $D \times D$ square grids each with length Δ_{D}. For simplicity, we assume $\mathcal{U}$ is an L m $\times L$ m square region and $D = \frac{L}{\Delta_{\mathrm{D}}}$. The quantization granularity Δ_{D} is selected as a sufficiently small value such that the large-scale channel gain and consequently the expected SNR remains approximately constant in each grid. Thus, all locations in each (i, j)-th grid can be well-represented by the grid center (or "grid point") denoted by $\boldsymbol{u}_{\mathrm{D}}(i, j) = [i - \frac{1}{2}, j - \frac{1}{2}]^T \Delta_{\mathrm{D}},\ i, j \in \mathcal{D}$ with $\mathcal{D} = \{1, \cdots, D\}$. Based on this, we can use a $D \times D$ matrix to store the expected SNR values at all grid points denoted by $\boldsymbol{S} \in \mathbb{R}^{D\times D}$, where each (i, j)-th element is given by $[\boldsymbol{S}]_{i,j} = \bar{\rho}(\boldsymbol{u}_{\mathrm{D}}(i, j)) = \max_{m\in\mathcal{M}} \frac{P_m \bar{g}_m^2(\boldsymbol{u}_{\mathrm{D}}(i,j))}{\sigma^2},\ i, j \in \mathcal{D}$. It is worth noting that $\boldsymbol{S}$ can be efficiently obtained via measurement or ray-tracing methods prior to the UAV's flight [19]. By depicting $\boldsymbol{S}$ for all grid points (i.e., all $i, j \in \mathcal{D}$), we have a so-called *expected SNR map*. In Fig. 2.1, we illustrate an expected SNR map under the setup in Section V.

Based on the above and by noting that Δ_{D} is sufficiently small, we propose a *discretized trajectory structure* for the UAV. Specifically, the path of the UAV

[1] Note that in $\rho_m(\boldsymbol{u})$, we did not consider real-time beamforming at the GBS/UAV based on the instantaneous small-scale channel. If such beamforming is considered, $\rho_m(\boldsymbol{u})$ and the expected SNR can be further improved; the expected SNR is still guaranteed to be higher than the required threshold $\bar{\rho}$.

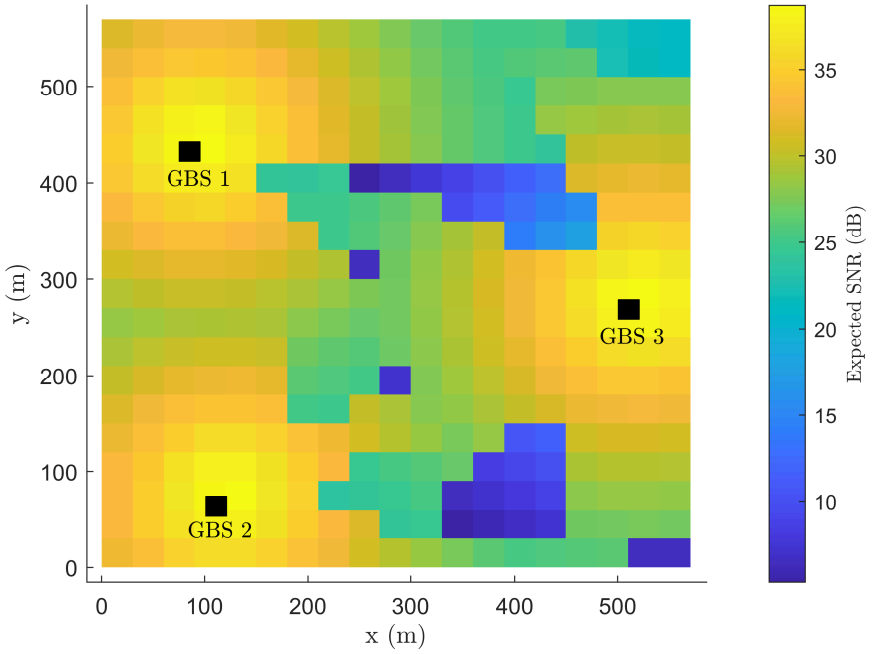

Figure 2.1: Illustration of an expected SNR map $\boldsymbol{S}$.

is composed of connected line segments, where the two end points of each line segment are two adjacent grid points, i.e., those with a distance no larger than $\sqrt{2}\Delta_{\mathrm{D}}$. Therefore, the UAV's trajectory can be represented by a series of grid points $\{\boldsymbol{u}_{\mathrm{D}}(i_n, j_n)\}_{n=1}^{N_{\mathrm{S}}}$, where $i_n, j_n \in \mathcal{D}$ and N_{S} denotes the total number of points. Consequently, to satisfy the expected SNR constraint, $[\boldsymbol{S}]_{i_n,j_n} \geq \bar{\rho}$, $\forall n$ should hold. Note that as $\Delta_{\mathrm{D}} \to 0$, the discretized trajectory approaches the continuous trajectory.

2.3.2 Target Sensing Model

In the target sensing mission, the UAV aims to sense the location of a target on the ground. Specifically, the horizontal location of the target denoted by $\boldsymbol{u}_{\mathrm{T}} = [x_{\mathrm{T}}, y_{\mathrm{T}}]^T$ is *unknown* and *random*, while its spatial distribution over the two-dimensional (2D) space is known *a priori* for exploitation, which can be obtained based on empirical data or target movement pattern. Let $p_{x_{\mathrm{T}},y_{\mathrm{T}}}(x_t, y_t)$ denote the probability density function (PDF) for the target's horizontal location $\boldsymbol{u}_{\mathrm{T}}$, where $[x_t, y_t]^T \in \mathcal{U}$. We assume that the UAV is able to sense the

target if the target's horizontal location lies in the same grid as the UAV, i.e., $|\boldsymbol{u}_{\mathrm{D}}(i_n, j_n) - \boldsymbol{u}_{\mathrm{T}}| \preceq [\frac{\Delta_{\mathrm{D}}}{2}, \frac{\Delta_{\mathrm{D}}}{2}]^T$.[2] In this case, the probability for the UAV to sense a target when it is located at $\boldsymbol{u}_{\mathrm{D}}(i_n, j_n)$ is given by the integral of the probabilities over all possible target locations in the corresponding grid, namely, $\int_{(i_n-1)\Delta_{\mathrm{D}}}^{i_n\Delta_{\mathrm{D}}} \int_{(j_n-1)\Delta_{\mathrm{D}}}^{j_n\Delta_{\mathrm{D}}} p_{x_{\mathrm{T}},y_{\mathrm{T}}}(x_t, y_t) dy_t dx_t$.

We aim to design the UAV's trajectory to maximize the *total probability* of sensing the target during the flight, which is given by

$$\sum_{n=1}^{N_{\mathrm{S}}} \int_{(i_n-1)\Delta_{\mathrm{D}}}^{i_n\Delta_{\mathrm{D}}} \int_{(j_n-1)\Delta_{\mathrm{D}}}^{j_n\Delta_{\mathrm{D}}} p_{x_{\mathrm{T}},y_{\mathrm{T}}}(x_t, y_t) dy_t dx_t. \tag{2.1}$$

To this end, we introduce a *target location distribution map*, which is represented by a matrix denoted by $\boldsymbol{P} \in \mathbb{R}^{D\times D}$ consisting of the target appearance probabilities and equivalently sensing probabilities in all $D \times D$ grids. Specifically, each (i, j)-th element in $\boldsymbol{P}$ is given by

$$[\boldsymbol{P}]_{i,j} = \int_{(i-1)\Delta_{\mathrm{D}}}^{i\Delta_{\mathrm{D}}} \int_{(j-1)\Delta_{\mathrm{D}}}^{j\Delta_{\mathrm{D}}} p_{x_{\mathrm{T}},y_{\mathrm{T}}}(x_t, y_t) dy_t dx_t, \ i, j \in \mathcal{D}. \tag{2.2}$$

Hence, the total sensing probability during the UAV's flight is $\sum_{n=1}^{N_{\mathrm{S}}} [\boldsymbol{P}]_{i_n,j_n}$. By further noting that visiting a grid point more than once is not beneficial to sensing, communication, or mission completion performance, we consider a non-repeated flight where each grid point is visited at most once, i.e., $\boldsymbol{u}_{\mathrm{D}}(i_n, j_n) \neq \boldsymbol{u}_{\mathrm{D}}(i_m, j_m), \ \forall n \neq m, \ n, m \in \mathcal{N} \triangleq \{1, \cdots, N_{\mathrm{S}}\}$.

Remark (Example of a Target Location Distribution): A practical target location distribution model is the 2D Gaussian mixture model, where the PDF

[2]Note that this model is applicable to various sensing methods. For camera-based sensing where the UAV senses a target by capturing video/image of it, this can guarantee a sufficiently high resolution. For radar sensing where the UAV is equipped with multiple antennas that constitute multiple-input multiple-output (MIMO) radar over non-overlapping frequency bands with GBS-UAV communication, this can guarantee that the received echo signal has sufficiently strong power, which leads to a sufficiently low sensing mean-squared error (MSE). It is also worth noting that the sensing accuracy can always be improved with a smaller grid granularity, such that the UAV is closer to the continuous locations in a grid, at a cost of higher complexity in map storage and trajectory optimization.

is the weighted sum of $S \geq 1$ 2D Gaussian PDFs, each with mean (x_s, y_s), variance σ_s^2, and weight $p_s \in [0, 1]$ that satisfies $\sum_{s=1}^{S} p_s = 1$, namely, $p_{x_\mathrm{T}, y_\mathrm{T}}(x_t, y_t) = \sum_{s=1}^{S} \frac{p_s}{2\pi\sigma_s^2} e^{-\frac{(x_t - x_s)^2 + (y_t - y_s)^2}{2\sigma_s^2}}$. In Fig. 2.2, we illustrate a target location distribution map $\boldsymbol{P}$ under this model, with $\Delta_\mathrm{D} = 30$ m, $p_1 = p_2 = 0.5$, $\sigma_1 = 1.8\Delta_\mathrm{D}$, $\sigma_2 = 2\Delta_\mathrm{D}$, $(x_1, y_1) = (13\Delta_\mathrm{D}, 5\Delta_\mathrm{D})$, and $(x_2, y_2) = (6\Delta_\mathrm{D}, 15\Delta_\mathrm{D})$.

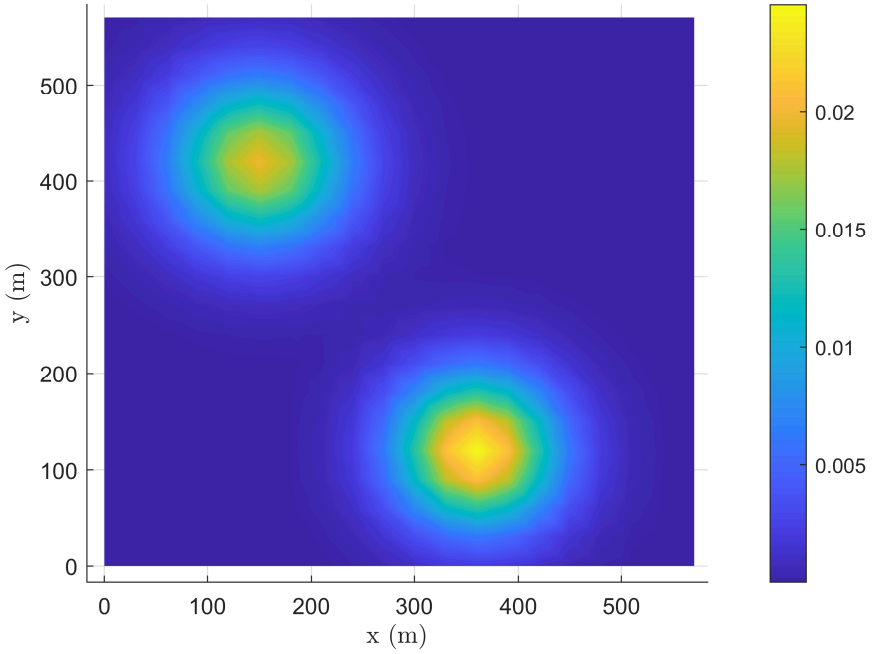

Figure 2.2: Illustration of a target location distribution map $\boldsymbol{P}$.

2.4. Problem Formulation

We aim to optimize the UAV's trajectory to maximize the total sensing probability, subject to an expected SNR constraint at each time instant during the flight and a maximum flying distance constraint. For ease of exposition, we assume that $\boldsymbol{u}_\mathrm{S} \triangleq [x_\mathrm{S}, y_\mathrm{S}]^T$ and $\boldsymbol{u}_\mathrm{F} \triangleq [x_\mathrm{F}, y_\mathrm{F}]^T$ are grid points.[3] Under the discretized trajectory structure, the problem is formulated as

[3]If $\boldsymbol{u}_\mathrm{S}$ and $\boldsymbol{u}_\mathrm{F}$ are not grid points, we can let the UAV firstly fly to the nearest grid point from $\boldsymbol{u}_\mathrm{S}$ and lastly fly from the nearest grid point to $\boldsymbol{u}_\mathrm{F}$.

$$\text{(P1)} \quad \max_{\{i_n,j_n\}_{n=1}^{N_\mathrm{S}}} \ \sum_{n=1}^{N_\mathrm{S}} [\boldsymbol{P}]_{i_n,j_n} \tag{2.3}$$

$$\text{s.t.} \quad \boldsymbol{u}_\mathrm{D}(i_1,j_1) = \boldsymbol{u}_\mathrm{S}, \boldsymbol{u}_\mathrm{D}(i_N,j_N) = \boldsymbol{u}_\mathrm{F} \tag{2.4}$$

$$[\boldsymbol{S}]_{i_n,j_n} \geq \bar{\rho}, \ \forall n \in \mathcal{N} \tag{2.5}$$

$$\sum_{n=1}^{N_\mathrm{S}-1} |\boldsymbol{u}_\mathrm{D}(i_{n+1},j_{n+1}) - \boldsymbol{u}_\mathrm{D}(i_n,j_n)\| \leq \bar{D} \tag{2.6}$$

$$\|\boldsymbol{u}_\mathrm{D}(i_{n+1},j_{n+1}) - \boldsymbol{u}_\mathrm{D}(i_n,j_n)\| \leq \sqrt{2}\Delta_\mathrm{D}, \ \forall n \in \mathcal{N} \tag{2.7}$$

$$\boldsymbol{u}_\mathrm{D}(i_n,j_n) \neq \boldsymbol{u}_\mathrm{D}(i_m,j_m), \ \forall n \neq m, \ n,m \in \mathcal{N} \tag{2.8}$$

$$i_n, j_n \in \mathcal{D}, \ \forall n \in \mathcal{N}. \tag{2.9}$$

In detail, constraint (2.4) specifies the initial and final locations; constraint (2.5) represents the expected SNR constraint, where each grid point in any feasible trajectory should satisfy the constraint (2.5) to ensure flight safety; constraint (2.6) gives a maximum flight distance constraint based on the consideration of energy or mission requirements; constraint (2.7) defines the discretized structure of the trajectory; and a non-repetitive flight trajectory is considered in constraint (2.8). Note that (P1) is a non-convex combinatorial optimization problem due to the integer optimization variables in $\{i_n, j_n\}_{n=1}^{N_\mathrm{S}}$. Moreover, (P1) is a constrained longest path problem, which can be shown to be NP-hard [80]. Particularly, note that to achieve a high total sensing probability, the optimal trajectory needs to traverse all grid points, which may lead to unaffordable flying distance. On the other hand, a trajectory that solely aims to traverse grid points with high sensing probabilities may be infeasible due to the expected SNR constraint. To summarize, the optimal trajectory needs to strike the best balance among the total probability, expected SNR, and flying distance, which makes (P1) very difficult to solve.

2.5. Proposed Solutions

2.5.1 Graph-based Problem Reformulation

To overcome the above challenges in solving (P1), we first propose to replace the objective function of (P1) with a lower bound of it given by

$$\sum_{n=1}^{N_{\mathrm{S}}}[\boldsymbol{P}]_{i_n,j_n} \geq 1/\left(\sum_{n=1}^{N_{\mathrm{S}}} 1/[\boldsymbol{P}]_{i_n,j_n}\right), \tag{2.10}$$

where the inequality holds due to the relationship between geometric mean and arithmetic mean.[4] Since (P1) is a constrained longest path problem, there is no efficient algorithm to solve it, to the best of our knowledge. To make the problem (P1) more tractable, we employ a lower bound of (P1) to find a suboptimal solution to (P1). Based on this, we transform (P1) into (P2) below:

$$\begin{aligned}
(\mathrm{P2}) \quad \min_{\{i_n,j_n\}_{n=1}^{N_{\mathrm{S}}}} \quad & \sum_{n=1}^{N_{\mathrm{S}}} 1/[\boldsymbol{P}]_{i_n,j_n} && (2.11)\\
\text{s.t.} \quad & \boldsymbol{u}_{\mathrm{D}}(i_1,j_1)=\boldsymbol{u}_{\mathrm{S}}, \boldsymbol{u}_{\mathrm{D}}(i_N,j_N)=\boldsymbol{u}_{\mathrm{F}} && (2.12)\\
& [\boldsymbol{S}]_{i_n,j_n} \geq \bar{\rho},\ \forall n \in \mathcal{N} && (2.13)\\
& \sum_{n=1}^{N_{\mathrm{S}}-1} |\boldsymbol{u}_{\mathrm{D}}(i_{n+1},j_{n+1}) - \boldsymbol{u}_{\mathrm{D}}(i_n,j_n)\| \leq \bar{D} && (2.14)\\
& \|\boldsymbol{u}_{\mathrm{D}}(i_{n+1},j_{n+1}) - \boldsymbol{u}_{\mathrm{D}}(i_n,j_n)\| \leq \sqrt{2}\Delta_{\mathrm{D}},\ n \in \mathcal{N} && (2.15)\\
& \boldsymbol{u}_{\mathrm{D}}(i_n,j_n) \neq \boldsymbol{u}_{\mathrm{D}}(i_m,j_m),\ \forall n \neq m,\ n,m \in \mathcal{N} && (2.16)\\
& i_n,j_n \in \mathcal{D},\ \forall n \in \mathcal{N}. && (2.17)
\end{aligned}$$

Next, we propose a graph-based model for (P2). Specifically, we construct an undirected weighted graph $G=(V,E)$ with two sets of weights. The vertex

[4] If $[\boldsymbol{P}]_{i,j}=0$, we can assign a small value to $[\boldsymbol{P}]_{i,j}$ to make it invertible.

set V is given by

$$V = \{U_{\mathrm{D}}(i,j) : [\boldsymbol{S}]_{i,j} \geq \bar{\rho},\ i,j \in \mathcal{D}\}, \tag{2.18}$$

where $U_{\mathrm{D}}(i,j)$ denotes the (i,j)-th grid point at location $\boldsymbol{u}_{\mathrm{D}}(i,j)$ that satisfies the expected SNR constraint. The edge set E is given below for $(i,j) \neq (k,l)$:

$$E = \{(U_{\mathrm{D}}(i,j), U_{\mathrm{D}}(k,l)) : \|\boldsymbol{u}_{\mathrm{D}}(i,j) - \boldsymbol{u}_{\mathrm{D}}(k,l)\| \leq \sqrt{2}\Delta_{\mathrm{D}}\}, \tag{2.19}$$

where an edge exists between two vertices if and only if they are adjacent. For each edge, we have a *distance weight* given below which represents the distance between two locations:

$$W^{\mathrm{D}}\left(U_{\mathrm{D}}(i,j), U_{\mathrm{D}}(k,l)\right) = \|\boldsymbol{u}_{\mathrm{D}}(i,j) - \boldsymbol{u}_{\mathrm{D}}(k,l)\|. \tag{2.20}$$

We also have a *probability weight* which denotes the inverse of sensing probability at the location of the latter vertex:

$$W^{\mathrm{P}}\left(U_{\mathrm{D}}(i,j), U_{\mathrm{D}}(k,l)\right) = 1/[\boldsymbol{P}]_{k,l}. \tag{2.21}$$

Note that any path in G from $U_{\mathrm{D}}(i_1,j_1)$ to $U_{\mathrm{D}}(i_{N_{\mathrm{S}}}, j_{N_{\mathrm{S}}})$ can be characterized by a $2 \times N_{\mathrm{S}}$ matrix $\boldsymbol{I} = [[i_1,j_1]^T, [i_2,j_2]^T, \cdots, [i_{N_{\mathrm{S}}}, j_{N_{\mathrm{S}}}]^T]$, for which the corresponding trajectory always satisfies the expected SNR constraint. The sum flying distance of $\boldsymbol{I}$ is given by

$$f^{\mathrm{D}}(\boldsymbol{I}) = \sum_{n=1}^{N_{\mathrm{S}}-1} W^{\mathrm{D}}(U_{\mathrm{D}}(i_n,j_n), U_{\mathrm{D}}(i_{n+1},j_{n+1})). \tag{2.22}$$

The sum sensing probability inverse of $\boldsymbol{I}$ is given by

$$f^{\mathrm{P}}(\boldsymbol{I}) = \frac{1}{[\boldsymbol{P}]_{i_1,j_1}} + \sum_{n=1}^{N_{\mathrm{S}}-1} W^{\mathrm{P}}(U_{\mathrm{D}}(i_n, j_n), U_{\mathrm{D}}(i_{n+1}, j_{n+1})). \tag{2.23}$$

Therefore, (P2) is equivalent to the following problem:

$$\text{(P3)} \min_{\boldsymbol{I}: f^{\mathrm{D}}(\boldsymbol{I}) \leq \bar{D}} f^{\mathrm{P}}(\boldsymbol{I}). \tag{2.24}$$

The feasibility for (P3) and consequently (P2) and (P1) can be checked by finding the shortest path from $U_{\mathrm{D}}(i_1, j_1)$ to $U_{\mathrm{D}}(i_{N_{\mathrm{S}}}, j_{N_{\mathrm{S}}})$ with respect to the distance weight $f^{\mathrm{D}}(\boldsymbol{I})$ via the Dijkstra algorithm [81]. If the resulting minimum distance is no larger than $\bar{D}$, (P3) and (P1) are feasible. In the following, we study (P3) assuming it has been verified to be feasible.

Note that (P3) is still a non-convex problem due to the integer variables in $\boldsymbol{I}$. Moreover, it is a *constrained shortest path problem* which is also NP-hard [17]. Finding the optimal solution to (P3) via exhaustive search requires complexity $\mathcal{O}(D^2!)$, which is unaffordable even for moderate map size. In the following, we propose a low-complexity high-quality suboptimal solution to (P3) via graph theory and convex optimization, which is also a suboptimal solution to (P1).

2.5.2 Proposed Solution I

In this subsection, we employ the Lagrangian relaxation method to obtain a suboptimal solution to (P3). Specifically, the Lagrangian of (P3) is given by $\mathscr{L}(\boldsymbol{I}, \lambda) = f^{\mathrm{P}}(\boldsymbol{I}) + \lambda f^{\mathrm{D}}(\boldsymbol{I})$, where λ is the dual variable. The Lagrange dual function is then given by $g(\lambda) = \min_{\boldsymbol{I}} \mathscr{L}(\boldsymbol{I}, \lambda) = \min_{\boldsymbol{I}} f^{\mathrm{P}}(\boldsymbol{I}) + \lambda f^{\mathrm{D}}(\boldsymbol{I})$. Consequently, the dual problem is given by

$$\text{(P3-Dual)} \max_{\lambda \geq 0} \min_{\boldsymbol{I}} f^{\mathrm{P}}(\boldsymbol{I}) + \lambda f^{\mathrm{D}}(\boldsymbol{I}). \tag{2.25}$$

Note that the dual problem (P3-Dual) is a convex optimization problem. However, the duality gap between (P3) and (P3-Dual) is generally non-zero, due to the non-convexity of (P3). Inspired by [17] which deals with a similar problem, we propose to solve (P3-Dual) and further find a high-quality primal solution denoted by $\boldsymbol{I}_{\mathrm{I}}$ via subgradient-based method and K-shortest path algorithm [17]. The details of this algorithm can be found in [17]. Note that this algorithm is guaranteed to obtain a feasible solution to (P3) and (P1). The worst-case complexity of the algorithm can be shown to be $\mathcal{O}(D^8 \log^2 D^2 + D^6 K)$, which is significantly reduced compared to that for finding the optimal solution, $\mathcal{O}(D^2!)$ [17].

Note that due to the replacement of objective function in (P3), the optimal solutions to (P1) and (P3) may not be the same, which may also lead to a difference between proposed solution I to (P3) and the optimal solution to (P1). In the following, we aim to mitigate such difference by proposing two further-improved solutions tailored to the structure of (P1).

2.5.3 Proposed Solution II

Although proposed solution I provides a systematic approach of finding a feasible solution to (P1), the minimizing nature of the transformed problem (P3) tends to reduce the number of grids visited by the UAV, which may limit the total sensing probability. For example, some grids with high sensing probabilities may be missed in proposed solution I.

To address this issue, we propose to utilize proposed solution I as an *initial trajectory*, and improve it by allowing the UAV to deviate from it at one waypoint and fly to a nearby grid point with high sensing probability before completing the flight. *Firstly*, we identify all the feasible grid points which satisfy the expected SNR constraint but were not selected in the initial trajectory and let V_{F} denote its set. *Secondly*, we sort them in a decreasing order of their

corresponding sensing probabilities, and select the top $R_{\mathrm{I}} \geq 1$ ones with the highest probabilities, which are denoted by $\{U_{\mathrm{D}}(k_r, l_r)\}_{r=1}^{R_{\mathrm{I}}}$ in graph G. *Thirdly*, for each $U_{\mathrm{D}}(k_r, l_r)$, we find its nearest location in the initial trajectory denoted by $U_{\mathrm{D}}(k'_r, l'_r)$ in G. Based on this, we propose a new trajectory for each r denoted by $\boldsymbol{I}_r$ that consists of three parts: 1) $U_{\mathrm{D}}(i_1, j_1)$ to $U_{\mathrm{D}}(k'_r, l'_r)$ same as the initial trajectory; 2) $U_{\mathrm{D}}(k'_r, l'_r)$ to $U_{\mathrm{D}}(k_r, l_r)$ as the shortest-distance trajectory under expected SNR constraint obtained via the Dijkstra algorithm over graph G; 3) $U_{\mathrm{D}}(k_r, l_r)$ to $U_{\mathrm{D}}(i_{N_{\mathrm{S}}}, j_{N_{\mathrm{S}}})$ as the shortest-distance trajectory under expected SNR constraint obtained via the Dijkstra algorithm over graph G. For each $\boldsymbol{I}_r$, we obtain the sum flying distance $f^{\mathrm{D}}(\boldsymbol{I}_r)$ according to (2.22). If we cannot find a trajectory that satisfies the above requirements, we set $f^{\mathrm{D}}(\boldsymbol{I}_r) = \infty$. *Finally*, among all $\boldsymbol{I}_r$'s and the initial trajectory $\boldsymbol{I}_{\mathrm{I}}$, we select the best trajectory as the one with a sum flying distance no larger than $\bar{D}$ and a maximum total sensing probability (the original objective function of (P1)). The obtained solution denoted by $\boldsymbol{I}_{\mathrm{II}}$ (proposed solution II) is guaranteed to achieve no smaller total sensing probability compared to $\boldsymbol{I}_{\mathrm{I}}$ due to the above selection procedure. The worst-case complexity for obtaining $\boldsymbol{I}_{\mathrm{II}}$ based on $\boldsymbol{I}_{\mathrm{I}}$ can be shown to be $\mathcal{O}(D^2 + R_{\mathrm{I}}(2D^4))$. Note that as R_{I} increases, the performance will increase at a cost of higher complexity. Thus, the value of R_{I} can be flexibly chosen according to practical requirements.

2.5.4 Proposed Solution III

In proposed solution III, we further enhance the performance by including *multiple* extra waypoints and allowing more flexible waypoint visiting order. Consider proposed solution I as the *initial trajectory*. *Firstly*, we select the top $R_{\mathrm{II}} \geq 1$ feasible grid points in V_{F} with the highest probabilities. *Secondly*, we aim to construct a new trajectory from the initial location $U_{\mathrm{D}}(i_1, j_1)$ to the final location $U_{\mathrm{D}}(i_{N_{\mathrm{S}}}, j_{N_{\mathrm{S}}})$ in G which traverses all waypoints in the initial trajectory and

all $R_{\rm II}$ new points with highest sensing probabilities. In light of the maximum flying distance constraint, this trajectory is designed to minimize the sum flying distance, which corresponds to a traveling salesman problem (TSP). Although TSP is an NP-hard problem, various algorithms have been developed for finding a high-quality suboptimal solution, such as the ant colony optimization (ACO) algorithm. Let $\boldsymbol{I}_{R_{\rm II}}$ denote the obtained trajectory with $R_{\rm II}$ more waypoints. If no feasible $\boldsymbol{I}_{R_{\rm II}}$ exists or $f^{\rm D}(\boldsymbol{I}_{R_{\rm II}}) > \bar{D}$, we will repeat the above procedures by incorporating one fewer, i.e., $R_{\rm II} - 1$, new waypoints with highest sensing probabilities, until a feasible solution is obtained or the number of new waypoints is reduced to zero (i.e., the trajectory is the same as the initial trajectory). The resulting proposed solution III denoted by $\boldsymbol{I}_{\rm III}$ is guaranteed to achieve no smaller total sensing probability than the initial trajectory due to the above selection procedure. The worst-case complexity for proposed solution III via ACO for TSP can be shown to be $\mathcal{O}(R_{\rm II}(CA(R_{\rm II}+N)^2 + (R_{\rm II}+N)D^4) + (R_{\rm II}+N)^2D^4)$, where C is the number of iterations and A is the number of ants in ACO.

2.6. Numerical Results

We consider a scenario shown in Fig. 2.3, with $L = 600$ m and $M = 3$ GBSs which have common height of 10 m and same transmit power of $P_m = 25$ dBm, $\forall m$. The large-scale channel is modeled under the urban micro (UMi) setup specified in 3GPP. The UAV flies at an altitude of $H = 80$ m and has an average receiver noise power of $\sigma^2 = -90$ dBm. The grid granularity is set as $\Delta_{\rm D} = 30$ m if not specified otherwise. The expected SNR map is shown in Fig. 2.1. For the target location distribution, we consider a truncated version of the map shown in Fig. 2.2 under Gaussian mixture PDF. Specifically, we remove the grids with obstacles and normalize the sensing probabilities of the entire area such that the sum sensing probabilities over all grids that do not overlap with obstacles is still

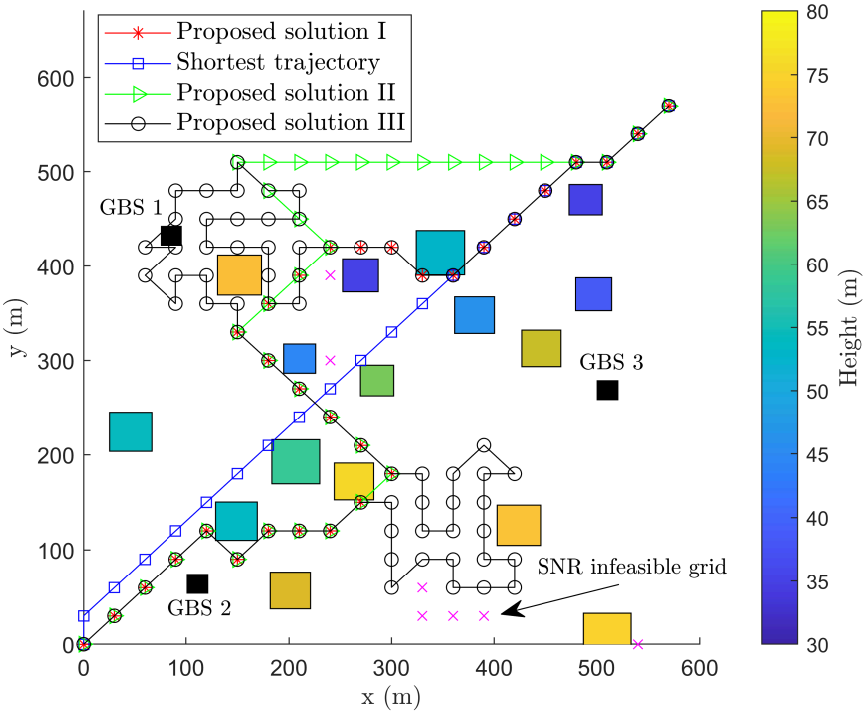

Figure 2.3: Illustration of trajectory designs with $\bar{D} = 2700$ m, $\Delta_{\mathrm{D}} = 30$ m.

1. We consider an expected SNR target of $\bar{\rho} = 7$ dB, under which the infeasible grid points are shown in Fig. 2.3. We consider a benchmark scheme where the UAV flies in the *shortest-distance trajectory* under the expected SNR constraint, without considering the sensing probability [19].

In Fig. 2.3, we show the trajectory designs via our proposed solutions I, II, III and the benchmark scheme under $\bar{D} = 2700$ m. It is observed that our proposed solutions tend to traverse grids with high sensing probabilities at the cost of higher flying distance compared to the benchmark scheme. In Fig. 2.4, we show the total sensing probability versus the maximum flying distance $\bar{D}$ for the aforementioned schemes, as well as proposed solutions II and III with the benchmark scheme (shortest-distance trajectory) as the initial trajectory. It is observed that all the proposed solutions outperform the benchmark scheme, and both proposed solutions II and III outperform proposed solution I due to the further improvements. Moreover, when the flying distance constraint is tight (i.e., $\bar{D}$ is small), proposed solution II outperforms proposed solution III since

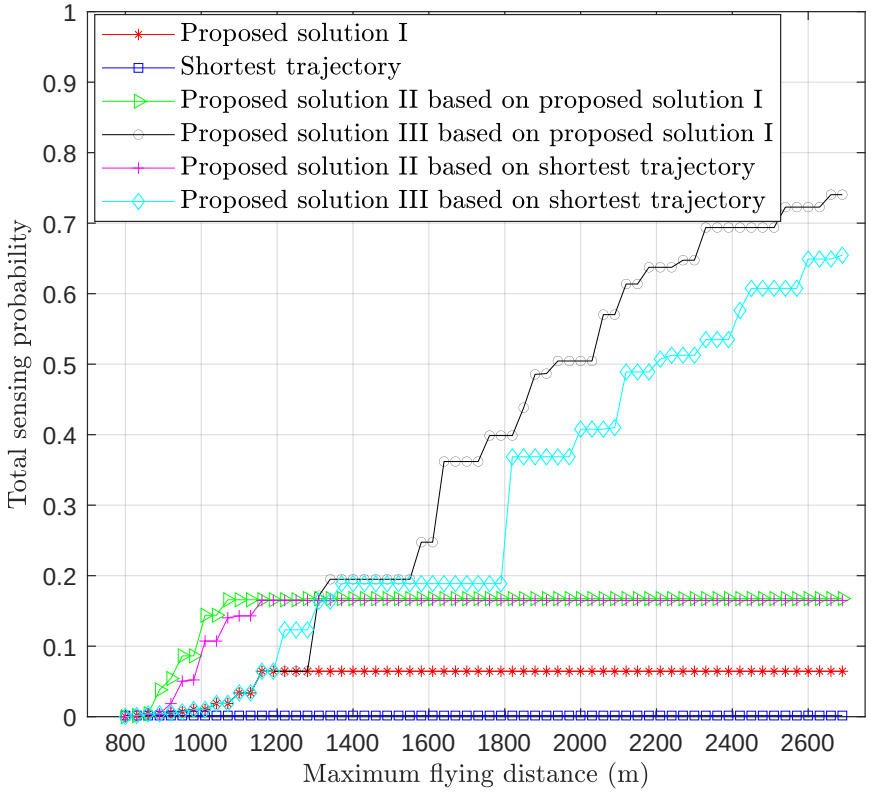

Figure 2.4: Illustration of total sensing probability versus $\bar{D}$ with $\Delta_{\mathrm{D}} = 30$ m.

the limited flying distance may not allow the inclusion of many high-probability locations; while when the flying distance constraint becomes relaxed (i.e., $\bar{D}$ is large), proposed solution III outperforms proposed solution II since it incorporates more high-probability locations with flexible visiting order design. In this setup, proposed solution III can improve the overall probability from 0.1649 (proposed solution II) to 0.7404 with $\bar{D} = 2700$ m. Finally, it is observed that for proposed solutions II and III, using proposed solution I as the initial trajectory generally leads to improved performance compared with using the shortest-distance trajectory, due to the joint consideration of the sensing probability and flying distance via the Lagrange relaxation method. In addition, we evaluate the performance under $\Delta_{\mathrm{D}} = 60$ m in Fig. 2.5, where the performance is observed to be worse than the case with $\Delta_{\mathrm{D}} = 30$ m. In Fig. 2.6, we show the computation time of different designs, where the case with $\Delta_{\mathrm{D}} = 60$ m is observed to consume less computation time, thus validating the performance-complexity trade-off in

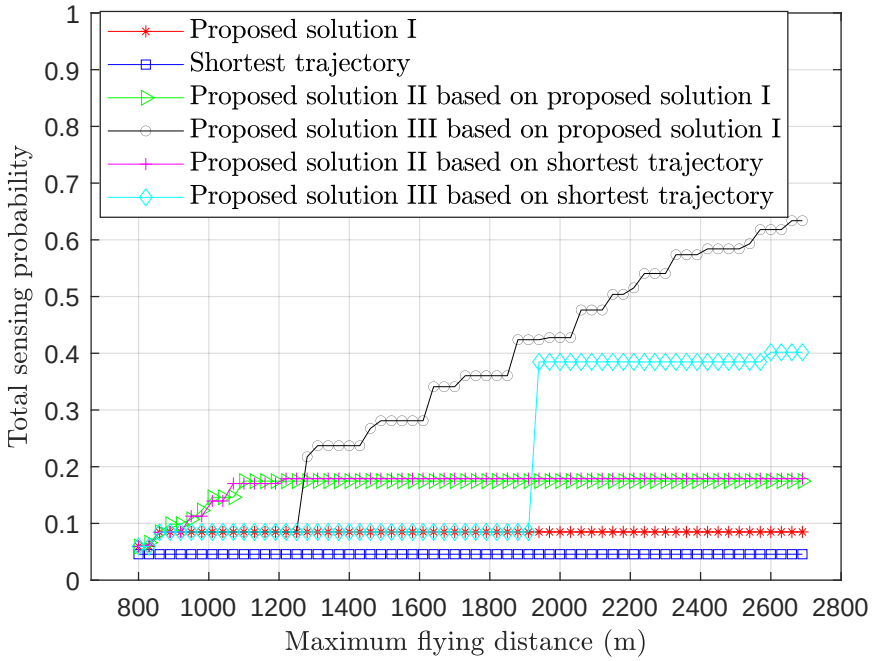

Figure 2.5: Illustration of total sensing probability versus $\bar{D}$ with $\Delta_{\mathrm{D}} = 60$ m.

selecting Δ_{D}.

2.7. Chapter Summary

In this chapter, we studied the trajectory optimization of a cellular-connected UAV in a sensing mission. Under a challenging scenario where the location of the target is unknown and random, we quantified the successful sensing probability at each possible UAV location, and further studied the trajectory optimization problem to maximize the total sensing probability over the flight, subject to a communication quality constraint and a mission completion time constraint. To achieve the challenges in solving this constrained longest path problem, we transferred the problem into a more trackable form by utilizing a lower bound of the objective function. Based on graph theory and Lagrangian relaxation techniques, we designed an effective algorithm to find an approximate solution. To close the optimal solution to the initial problem, we proposed two solutions to further enhance the performance. Numerical results showed that the UAV's

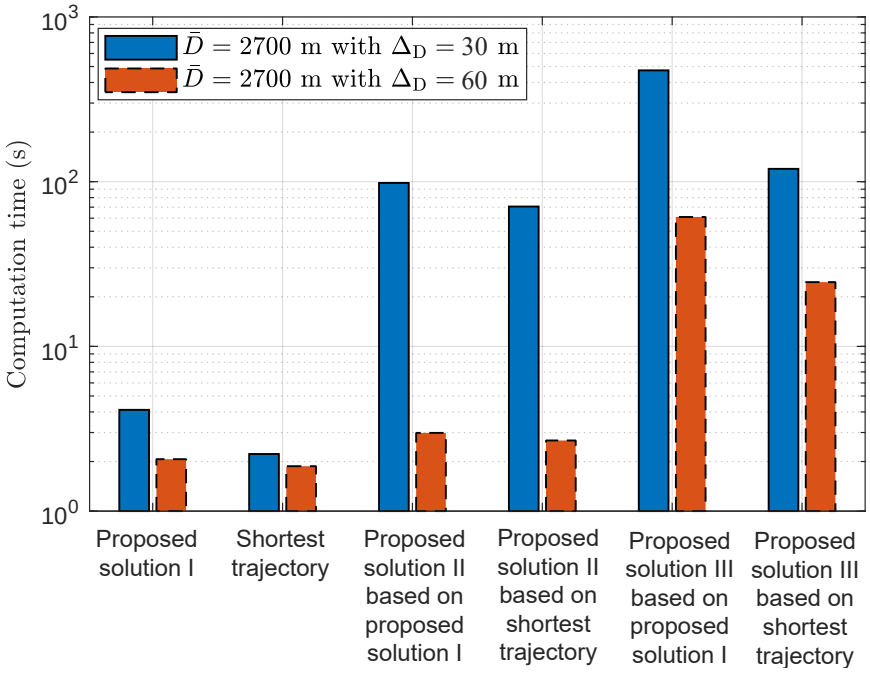

Figure 2.6: Illustration of computation time with $\bar{D} = 2700$ m.

trajectories are numerically verified, and our proposed solutions significantly increase the overall probability compared with benchmark schemes.

3. Handover-Aware Trajectory Optimization for Cellular-Connected UAV

3.1. Introduction

In this chapter, we study a cellular-connected UAV which aims to complete a mission of flying between two pre-determined locations while maintaining satisfactory communication quality with the ground base stations (GBSs). Due to the potentially long distance of the UAV's flight, frequent handovers may be incurred among different GBSs, which leads to various practical issues such as large delay and synchronization overhead. To address this problem, we investigate the trajectory optimization of the UAV to minimize the number of GBS handovers during the flight, subject to a communication quality constraint and a maximum mission completion time constraint. Although this problem is non-convex and difficult to solve, we derive useful structures of the optimal solution, based on which we propose an efficient algorithm based on graph theory and Lagrangian relaxation for finding a high-quality suboptimal solution in polynomial time. Numerical results validate the effectiveness of our proposed trajectory design.

The remainder of this chapter is organized as follows. Section 3.2 presents

a literature review. Section 3.3 introduces the system model for a cellular-connected UAV and formulates the handover function. Section 3.4 presents this trajectory optimization problem. Section 3.5 proposes some structural properties for the optimal UAV trajectory, and reformulates a more tractable problem. Section 3.6 proposes a high-quality solution. Numerical results are provided in Section 3.7 to evaluate the performance of proposed solutions. Finally, Section 3.8 concludes the chapter.

3.2. Literature Review

As UAVs operate in dynamic environments and often move across wide geographical areas, effective handover mechanisms are crucial to maintaining seamless communication, especially when they rely on heterogeneous cellular networks. This literature review examines the existing research on UAV handover management.

Handover mechanisms can be broadly categorized based on their operational strategies, including hard handover and soft handover. [64–66] studied those handover mechanisms and their performance analysis for UAV communication. Moreover, handover mechanisms rely on various communication protocols to manage the transition between service supporters. [67–69] proposed secure and efficient protocols for UAV communication. In addition, [61–63, 70] analyze the handover process and effection for UAV communication. Their research demonstrated that handover will affect the communication quality, including handover latency, packet loss, throughput, and signal strength.

Compared with other performance metrics such as the mission completion time, the number of handovers is a discrete-valued function that is difficult to be characterized explicitly with respect to the UAV's trajectory. Moreover, there exists non-trivial trade-offs among the handover performance, mission comple-

tion performance, and communication performance, which make handover-aware trajectory optimization more challenging. Note that existing works proposed new protocols and handover mechanisms to reduce the number of handovers and decrease the negative impact of the handovers. In practice, the decreased number of handovers can be achieved by optimizing UAVs' trajectory. However, how to design the UAV trajectory to minimize the total number of handovers has not been studied in the existing literature to our best knowledge.

3.3. System Model

We consider a cellular-enabled UAV communication system with $M \geq 1$ *heterogeneous* GBSs and a UAV. Both the UAV and each GBS are equipped with one single antenna.[1] We assume that the UAV flies at a constant height of H in meters (m), and its three-dimensional (3D) location at time instant t is denoted as $(x(t), y(t), H),\ 0 \leq t \leq T$. Specifically, T represents the completion time of the UAV's mission in seconds (s), which should be no longer than a predefined maximum mission completion time threshold $T_{\max}$. The mission of the UAV is to fly from an initial point U_0 to a final point $U_{\rm F}$, for which the locations are denoted by $[x_0, y_0, H]^T$ and $[x_{\rm F}, y_{\rm F}, H]^T$, respectively. During the flight, the UAV is required to maintain satisfactory downlink communication quality with the GBSs at every time instant.

We consider a *heterogeneous* network where each GBS may have a different antenna height and a different transmit power for downlink UAV communication. For each m-th GBS, we let H_m and P_m denote the antenna height and transmit power for UAV communication, respectively, and (a_m, b_m, H_m) denote its 3D location. For illustration, we further define $\boldsymbol{g}_m = [a_m, b_m]^T$ and $\boldsymbol{u}(t) = [x(t), y(t)]^T$ to represent the horizontal locations of each m-th GBS and

[1]It is worth noting that our results can be readily extended to the case with multiple antennas at the GBSs/UAV by re-quantifying the communication quality with multi-antenna gain/beamforming taken into account.

the UAV at time instant t, respectively. In addition, we define $\bar{\boldsymbol{u}}_0 = [x_0, y_0]^T$ and $\bar{\boldsymbol{u}}_{\rm F} = [x_{\rm F}, y_{\rm F}]^T$, with $\boldsymbol{u}(0) = \bar{\boldsymbol{u}}_0$ and $\boldsymbol{u}(T) = \bar{\boldsymbol{u}}_{\rm F}$. We consider a maximum speed constraint of the UAV denoted by $V_{\max}$, which yields $\|\dot{\boldsymbol{u}}(t)\| \leq V_{\max}$. The link distance between the m-th GBS and the UAV at each time instant t is given by $d_m(t) = \sqrt{(H - H_m)^2 + \|\boldsymbol{u}(t) - \boldsymbol{g}_m\|^2}$, $m \in \mathcal{M}$, where $\mathcal{M} = \{1, \cdots, M\}$. For ease of understanding the fundamental trade-offs among handover, mission completion time, and communication quality, we consider the LoS channel model between GBSs and the UAV. Let $h_m(t) \in \mathbb{C}$ denote the complex baseband equivalent channel coefficient from each m-th GBS to the UAV at time instant t. The corresponding channel power gain is modeled as $|h_m(t)|^2 = \frac{\beta_0}{d_m^2(t)} = \frac{\beta_0}{(H-H_m)^2+\|\boldsymbol{u}(t)-\boldsymbol{g}_m\|^2}$, $m \in \mathcal{M}$, where β_0 denotes the channel power gain at reference distance $d_0 = 1$ m. We assume that the UAV communicates with one GBS indexed by $I(t) \in \mathcal{M}$ at each time instant t, and a dedicated time-frequency resource block is allocated for UAV communication. The receive SNR at the UAV at time instant t is thus given by

$$\rho_{I(t)}(t) = \frac{P_{I(t)}\beta_0}{\sigma^2((H - H_{I(t)})^2 + \|\boldsymbol{u}(t) - \boldsymbol{g}_{I(t)}\|^2)}, \ 0 \leq t \leq T, \tag{3.1}$$

where σ^2 denotes the average noise power at the UAV receiver. We consider a communication quality requirement specified by a minimum receive SNR threshold denoted by $\bar{\rho}$. Namely, the UAV can satisfactorily communicate with GBS $I(t)$ at time instant t if and only if $\rho_{I(t)}(t) \geq \bar{\rho}$ or equivalently $\|\boldsymbol{u}(t) - \boldsymbol{g}_{I(t)}\| \leq \bar{d}_{I(t)} \triangleq \sqrt{\frac{P_{I(t)}\beta_0}{\sigma^2\bar{\rho}} - (H - H_{I(t)})^2}$ holds, i.e., the horizontal location of the UAV lies in the disk-shaped (horizontal) *coverage region* of GBS $I(t)$ centered at $\boldsymbol{g}_{I(t)}$ with radius $\bar{d}_{I(t)}$, as illustrated in Fig. 3.1.

Note that at each time instant t, there may exist multiple GBSs that can satisfy the communication constraint when associated with the UAV. However, frequent change of the GBS-UAV association $I(t)$ over time leads to frequent

GBS *handovers*, and consequently causes increased delay and overhead (e.g., for synchronization). Motivated by this, we aim to judiciously design the UAV's trajectory and GBS-UAV associations $I(t)$'s to minimize the total number of handovers during the UAV's mission, while maintaining satisfactory communication quality and mission completion time.

To this end, we first mathematically characterize the number of handovers. We consider that a handover happens when the UAV reaches the boundary of the coverage region of the GBS currently associated with the UAV, and is about to enter the coverage region of another GBS, as illustrated in Fig. 3.1. Specifically, define $\chi(t)$ to indicate whether the UAV has reached the boundary of the coverage region of the currently associated GBS:

$$\chi(t) = \sum_{t' \in \{\tau : \|\boldsymbol{u}(\tau) - \boldsymbol{g}_{I(\tau)}\| - \bar{d}_{I(\tau)} = 0,\ \tau \in [0,T]\}} \delta(t - t'),\ 0 \le t \le T, \tag{3.2}$$

where $\delta(\cdot)$ denotes the Dirac-delta function. Moreover, let $\psi(t)$ indicate whether the UAV is ready to enter the coverage region of another GBS, which is given by

$$\psi(t) = \begin{cases} 1, \text{ if } \min\limits_{m \in \mathcal{M} \backslash \{I(t)\}} \|\boldsymbol{u}(t) - \boldsymbol{g}_m\| - \bar{d}_m \le 0 \\ 0, \text{ otherwise} \end{cases},\ 0 \le t \le T. \tag{3.3}$$

Note that $\psi(t) = 1$ indicates that the UAV is ready to be associated with another GBS indexed by $m \in \mathcal{M} \backslash \{I(t)\}$ that is different from the associated one, and $\psi(t) = 0$ otherwise. Notice that $\chi(t)\psi(t)$ consists of multiple time-shifted Dirac-delta functions, each taking a non-zero value at a handover time instant. Therefore, the total number of handovers during the UAV's flight can be expressed as:

$$N = \int_0^T \chi(t)\psi(t)dt. \tag{3.4}$$

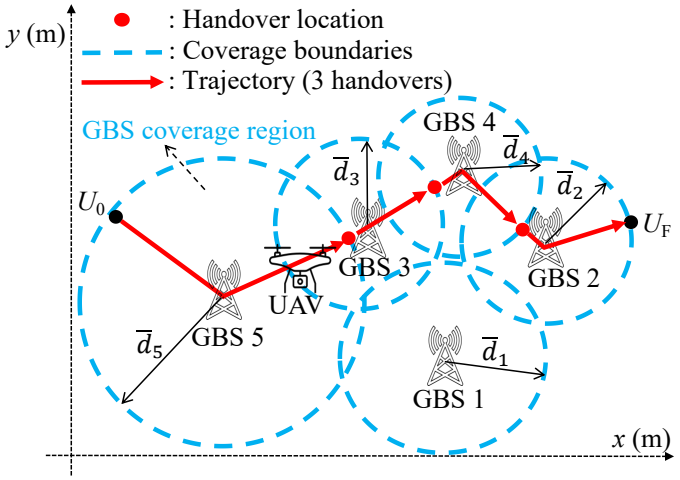

Figure 3.1: Illustration of handover locations for a cellular-connected UAV with different trajectories.

Note that the number of handovers in (3.4) is critically dependent on the UAV's trajectory $\{\boldsymbol{u}(t), 0 \leq t \leq T\}$ and GBS-UAV associations $\{I(t), 0 \leq t \leq T\}$, which also critically affect the communication quality and mission completion time. In general, there exists a non-trivial trade-off among the handover, communication, and mission completion performances. For example, to maximize the receive SNR, the UAV should fly near the GBSs during its flight as much as possible, which, on the other hand, may result in a large number of handovers and long mission completion time. To resolve this trade-off, we will jointly optimize the UAV's trajectory and GBS-UAV associations for minimizing the number of handovers subject to communication quality and mission completion requirements.

3.4. Problem Formulation

We aim to jointly optimize the UAV's trajectory $\{\boldsymbol{u}(t), 0 \leq t \leq T\}$ and the GBS-UAV associations $\{I(t), 0 \leq t \leq T\}$ to minimize the number of handovers, subject to a communication quality constraint specified by a minimum receive SNR threshold $\bar{\rho}$ and a maximum mission completion time threshold $T_{\max}$. The

optimization problem is formulated as

$$\text{(P1)} \quad \min_{\substack{T,\{\boldsymbol{u}(t),0\le t\le T\},\\ \{I(t),0\le t\le T\}}} \quad N \tag{3.5}$$

$$\text{s.t.} \quad \boldsymbol{u}(0)=\bar{\boldsymbol{u}}_0,\ \boldsymbol{u}(T)=\bar{\boldsymbol{u}}_{\mathrm{F}} \tag{3.6}$$

$$\|\boldsymbol{u}(t)-\boldsymbol{g}_{I(t)}\|-\bar{d}_{I(t)}\le 0,\ 0\le t\le T \tag{3.7}$$

$$I(t)\in\mathcal{M},\ 0\le t\le T \tag{3.8}$$

$$\|\dot{\boldsymbol{u}}(t)\|\le V_{\max},\ 0\le t\le T \tag{3.9}$$

$$T\le T_{\max}. \tag{3.10}$$

Note that the objective function defined in (3.4) is in a complex form which is a non-decreasing step function of the mission completion time T. Moreover, both $\boldsymbol{u}(t)$ and $I(t)$ are continuous functions over time. Thus, (P1) involves an infinite number of optimization variables. Furthermore, $I(t)$'s are discrete optimization variables and the objective function N is an integer-valued function. To summarize, (P1) is a non-convex optimization problem for which the optimal solution is difficult to obtain. Particularly, the new consideration of the number of handovers brings brand new challenges compared to existing works on the trajectory optimization for cellular-connected UAV (e.g., [15, 17, 19]). In the following, we will first transform the problem into a more tractable equivalent form by exploiting its structural properties.

3.5. Structural Properties of the Optimal Solution and Problem Reformulation

First, we introduce a set of auxiliary variables $\{T_i\}_{i=0}^{N}$, where $T_i,\ 1\le i\le N-1$, denotes the time duration between the i-th handover and the $(i+1)$-th handover; T_0 represents the time duration from the mission start to the first

handover; and T_N denotes the time duration from the N-th handover to the mission completion. Moreover, we let an auxiliary vector $\boldsymbol{I} = [I_0, \cdots, I_i, \cdots, I_N]^T$ with $I_i \in \mathcal{M},\ \forall i$ represent the *GBS-UAV association sequence*, where $I_0 = I(t),\ t \in [0, T_0]$, and $I_i = I(t),\ t \in \Big[\sum_{j=0}^{i-1} T_j, \sum_{j=0}^{i} T_j\Big],\ i = 1, \cdots, N$. Based on this, (P1) can be equivalently transformed into

$$\text{(P2)} \quad \min_{\substack{T, \{\boldsymbol{u}(t), 0 \le t \le T\}, \\ \boldsymbol{I}, \{T_i\}_{i=0}^N}} \quad N \tag{3.11}$$

$$\text{s.t.} \quad (3.6), (3.9), (3.10) \tag{3.12}$$

$$\|\boldsymbol{u}(t) - \boldsymbol{g}_{I_i}\| - \bar{d}_{I_i} \le 0,$$
$$t \in \left[\sum_{j=0}^{i-1} T_j, \sum_{j=0}^{i} T_j\right],\ i = 0, \cdots, N \tag{3.13}$$

$$I_i \in \mathcal{M},\ i = 0, \cdots, N. \tag{3.14}$$

Note that compared to (P1), (P2) replaces the continuous-time $I(t)$ with a discrete sequence $\boldsymbol{I}$, based on which the number of handovers can also be expressed as the cardinality of $\boldsymbol{I}$. However, there are still M^{N+1} possible solutions of $\boldsymbol{I}$, which motivates us to provide the following proposition.

Proposition 1 *The optimal number of handovers satisfies $N \le M - 1$. The optimal $\boldsymbol{I}$ to (P2) satisfies*

$$I_i \ne I_j,\ \forall i \ne j,\ i, j = 0, \cdots, N. \tag{3.15}$$

Proof: Consider a feasible trajectory to (P2) denoted by $\{\hat{\boldsymbol{u}}(t), 0 \le t \le \hat{T}\}$ with repeated GBS-UAV associations, where the association sequence is denoted by $\hat{\boldsymbol{I}} = [\hat{I}_0, \cdots, \hat{I}_k, \cdots, \hat{I}_q, \cdots, \hat{I}_{\hat{N}}]^T$ with $k < q$ and $\hat{I}_k = \hat{I}_q$. We prove Proposition 1 by showing that a new feasible trajectory can be constructed without repeated association and with reduced number of handovers. Specifically, we construct the GBS-UAV association sequence by removing the $(k+1)$-th to

the q-th elements in $\hat{\boldsymbol{I}}$, which is given by $\tilde{\boldsymbol{I}} = [\hat{I}_0, \cdots, \hat{I}_k, \hat{I}_{q+1}, \cdots, \hat{I}_{\hat{N}}]^T$. The new feasible trajectory is then constructed by replacing the part in the original trajectory from $\hat{\boldsymbol{u}}(\sum_{j=0}^{k} \hat{T}_j)$ to $\hat{\boldsymbol{u}}(\sum_{j=0}^{q-1} \hat{T}_j)$ (during which the UAV leaves the association with GBS $\hat{I}_k$ and becomes associated with it again) by a straight-line path with maximum speed from $\hat{\boldsymbol{u}}(\sum_{j=0}^{k} \hat{T}_j)$ to $\hat{\boldsymbol{u}}(\sum_{j=0}^{q-1} \hat{T}_j)$. Note that since $\hat{\boldsymbol{u}}(\sum_{j=0}^{k} \hat{T}_j)$ and $\hat{\boldsymbol{u}}(\sum_{j=0}^{q-1} \hat{T}_j)$ are both within the disk-shaped coverage region of GBS $\hat{I}_k$, the newly constructed trajectory satisfies the communication quality constraint. Moreover, the replaced part consumes no longer time compared to the original part, as it incurs shortest distance with maximum speed, thus the newly constructed trajectory satisfies the mission completion time constraint. Finally, the newly constructed trajectory yields a smaller number of handovers of $\tilde{N} = \hat{N} - q + k < \hat{N}$. This thus completes the proof of Proposition 1.

Proposition 1 indicates there should be no more than $M - 1$ handovers in the UAV's mission, and significantly reduces the feasible set of $\boldsymbol{I}$ based on (3.15). Furthermore, we let $\boldsymbol{u}_i = \boldsymbol{u}\Big(\sum_{j=0}^{i-1} T_j\Big)$ represent the location where the UAV is handed over from GBS $\boldsymbol{g}_{I_{i-1}}$ to GBS $\boldsymbol{g}_{I_i}$. For completeness, we define the initial location $\boldsymbol{u}_0 = \boldsymbol{u}(0) = \bar{\boldsymbol{u}}_0$ and the final location $\boldsymbol{u}_{N+1} = \boldsymbol{u}(T) = \bar{\boldsymbol{u}}_{\rm F}$. Based on $\{\boldsymbol{u}_i\}_{i=0}^{N+1}$ defined above, we propose the following proposition.

Proposition 2 *Without loss of optimality, the optimal solution to (P2) can be assumed to satisfy the following conditions:*

$$T_i = \frac{\|\boldsymbol{u}_{i+1} - \boldsymbol{u}_i\|}{V_{\max}},\ i = 0, \cdots, N \tag{3.16}$$

$$\boldsymbol{u}(t) = \boldsymbol{u}_i + \Big(t - \sum_{j=0}^{i-1} T_j\Big) V_{\max} \frac{\boldsymbol{u}_{i+1} - \boldsymbol{u}_i}{\|\boldsymbol{u}_{i+1} - \boldsymbol{u}_i\|},$$
$$t \in \left[\sum_{j=0}^{i-1} T_j, \sum_{j=0}^{i} T_j\right],\ i = 0, \cdots, N. \tag{3.17}$$

Proof: We prove Proposition 2 by showing that for any feasible solution to (P2) denoted by $(\hat{T}, \{\hat{\boldsymbol{u}}(t), 0 \le t \le \hat{T}\}, \boldsymbol{I}, \{\hat{T}_i\}_{i=0}^{N})$ that does not satisfy the

conditions in (3.16), (3.17), we can always construct a feasible solution to (P2) denoted by $(T, \{\boldsymbol{u}(t), 0 \le t \le T\}, \boldsymbol{I}, \{T_i\}_{i=0}^{N})$ that satisfies these conditions with the same objective value. We set the handover locations in $\{\boldsymbol{u}(t), 0 \le t \le T\}$ as the same ones in $\{\hat{\boldsymbol{u}}(t), 0 \le t \le \hat{T}\}$, i.e., $\boldsymbol{u}_i = \hat{\boldsymbol{u}}\Big(\sum_{j=0}^{i-1} \hat{T}_j\Big),\ i = 0, \cdots, N+1$. Based on this, the new solution is constructed based on (3.16), (3.17). Note that $\hat{T}_i$ denotes the time duration for the UAV to fly from $\boldsymbol{u}_{i+1}$ to $\boldsymbol{u}_i$, where $\hat{T}_i = \frac{\|\boldsymbol{u}_{i+1} - \boldsymbol{u}_i\|}{\|\dot{\hat{\boldsymbol{u}}}(t)\|}$, thus $\hat{T}_i \ge \frac{\|\boldsymbol{u}_{i+1} - \boldsymbol{u}_i\|}{V_{\max}}$ should hold due to the constraint in (3.9). By noting that $T_i = \frac{\|\boldsymbol{u}_{i+1} - \boldsymbol{u}_i\|}{V_{\max}}$, we have $T_i \le \hat{T}_i,\ i = 0, \cdots, N$, and consequently $T = \sum_{i=0}^{N} \frac{\|\boldsymbol{u}_{i+1} - \boldsymbol{u}_i\|}{V_{\max}} \le \hat{T} = \sum_{i=0}^{N} \frac{\|\boldsymbol{u}_{i+1} - \boldsymbol{u}_i\|}{\|\dot{\hat{\boldsymbol{u}}}(t)\|} \le T_{\max}$. Moreover, the newly constructed solution also satisfies the communication quality constraint since the line segment between two consecutive handover locations is guaranteed to lie in the disk-shaped GBS coverage region. Thus, the new solution is feasible for (P2) with unchanged objective value N, which completes the proof of Proposition 2.

Proposition 2 indicates that the optimal horizontal trajectory is composed of multiple connected line segments, and the UAV flies along these line segments at maximum speed $V_{\max}$. Specifically, the i-th line segment's start and end points are the $(i-1)$-th handover location $\boldsymbol{u}_{i-1}$ and the i-th handover location $\boldsymbol{u}_i$, respectively. Based on this, we equivalently transform (P2) and consequently

(P1) into the following problem:

$$\text{(P3)} \quad \min_{\{\boldsymbol{u}_i\}_{i=0}^{N+1}, \boldsymbol{I}} \quad N \tag{3.18}$$

$$\text{s.t.} \quad (3.6), (3.14), (3.15) \tag{3.19}$$

$$\boldsymbol{u}_0 = \bar{\boldsymbol{u}}_0, \ \boldsymbol{u}_{N+1} = \bar{\boldsymbol{u}}_{\mathrm{F}} \tag{3.20}$$

$$\sum_{i=0}^{N} \|\boldsymbol{u}_{i+1} - \boldsymbol{u}_i\| \leq T_{\max} V_{\max} \tag{3.21}$$

$$\|\boldsymbol{u}_i - \boldsymbol{g}_{I_i}\| \leq \bar{d}_{I_i}, \ i = 0, \cdots, N \tag{3.22}$$

$$\|\boldsymbol{u}_i - \boldsymbol{g}_{I_{i-1}}\| = \bar{d}_{I_{i-1}}, \ i = 1, \cdots, N \tag{3.23}$$

$$\|\boldsymbol{u}_{N+1} - \boldsymbol{g}_{I_N}\| \leq \bar{d}_{I_N}. \tag{3.24}$$

Note that in contrast to (P1), the equivalent problem (P3) is a joint optimization problem of the GBS-UAV association sequence and handover locations, which does not involve any continuous function over time. However, it is still a non-convex optimization problem due to the non-convex constraint in (3.23) and the discrete optimization variables in $\boldsymbol{I}$. In the following, we will leverage *graph theory* to handle (P3).

3.6. Proposed Solution to Problem (P3)

Note that a key difficulty in (P3) lies in the mixture of the continuous and discrete optimization variables representing the handover locations and GBS-UAV association sequence, respectively. To address this challenge, we first propose an effective structural design of the handover locations, based on which (P3) can be modeled and tackled via graph theory.

3.6.1 Handover Location Design

Motivated by Proposition 2 and the fact that the communication quality improves as the UAV flies closer to the GBS, we propose a structural handover location design. Specifically, the UAV firstly flies from the start location to the location on top of the firstly connected GBS. Then, the UAV flies in a straight line between the locations on top of the sequentially associated GBSs, where the i-th (horizontal) handover location $\boldsymbol{u}_i$ is located at the intersection of the line segment from the I_{i-1}-th to the I_i-th GBSs and the coverage boundary of the I_{i-1}-th GBS. Finally, the UAV flies from the location above the lastly associated GBS to the final destination, as illustrated in Fig. 3.1. We let $\tilde{T}_i,\ 1 \leq i \leq N$, represent the time duration for the UAV to fly between the locations on top of GBSs I_{i-1} and I_i; $\tilde{T}_0$ denote the time duration for the UAV to fly from the initial location to the location above the firstly associated GBS; $\tilde{T}_{N+1}$ denote the time duration for the UAV to fly from the location above the lastly associated GBS to the final destination. The UAV's trajectory and mission completion time are thus given by

$$\boldsymbol{u}(t) = \begin{cases} \boldsymbol{u}_0 + tV_{\max}\frac{\boldsymbol{g}_{I_0}-\boldsymbol{u}_0}{\|\boldsymbol{g}_{I_0}-\boldsymbol{u}_0\|},\ t \in [0, \tilde{T}_0] \\ \boldsymbol{g}_{I_0} + \Big(t - \sum\limits_{j=0}^{i}\tilde{T}_j\Big)V_{\max}\frac{\boldsymbol{g}_{I_{i+1}}-\boldsymbol{g}_{I_i}}{\|\boldsymbol{g}_{I_{i+1}}-\boldsymbol{g}_{I_i}\|}, \\ \quad t \in \Big[\sum\limits_{j=0}^{i}\tilde{T}_j, \sum\limits_{j=0}^{i+1}\tilde{T}_j\Big],\ i = 0, \cdots, N-1 \\ \boldsymbol{g}_{I_N} + \Big(t - \sum\limits_{j=0}^{N}\tilde{T}_j\Big)V_{\max}\frac{\boldsymbol{u}_{N+1}-\boldsymbol{g}_{I_N}}{\|\boldsymbol{u}_{N+1}-\boldsymbol{g}_{I_N}\|}, \\ \quad t \in \Big[\sum\limits_{j=0}^{N}\tilde{T}_j, T\Big] \end{cases}, \tag{3.25}$$

$$T = \frac{\|\boldsymbol{u}_0 - \boldsymbol{g}_{I_0}\|}{V_{\max}} + \frac{\|\boldsymbol{u}_{N+1} - \boldsymbol{g}_{I_N}\|}{V_{\max}} + \sum_{i=0}^{N-1}\frac{\|\boldsymbol{g}_{I_{i+1}} - \boldsymbol{g}_{I_i}\|}{V_{\max}}. \tag{3.26}$$

Based on the above handover location structure, (P3) can be transformed to the following problem:

$$\text{(P4)} \ \min_{\boldsymbol{I}} \ N \tag{3.27}$$

$$\text{s.t. } (3.6), (3.14), (3.15) \tag{3.28}$$

$$\|\boldsymbol{u}_0 - \boldsymbol{g}_{I_0}\| + \|\boldsymbol{u}_{N+1} - \boldsymbol{g}_{I_N}\| + \sum_{i=0}^{N-1} \|\boldsymbol{g}_{I_{i+1}} - \boldsymbol{g}_{I_i}\| \leq T_{\max} V_{\max} \tag{3.29}$$

$$\|\boldsymbol{g}_{I_i} - \boldsymbol{g}_{I_{i-1}}\| - \bar{d}_{I_i} - \bar{d}_{I_{i-1}} \leq 0, \ i = 1, \cdots, N. \tag{3.30}$$

Notice that the only variable in (P4) is the GBS-UAV association sequence $\boldsymbol{I}$, which should satisfy the constraint in (3.30) such that each pair of GBSs I_{i-1} and I_i can be consecutively associated with the UAV. Although the optimal solution to (P4) may not be optimal to (P3) and consequently (P1) due to the specific handover location design considered, it enables an equivalent graph-based modeling, as shown below.

3.6.2 Equivalent Graph-Based Model and Solution for (P4)

Note that an edge exists between two vertices if and only if their corresponding GBSs can be potentially consecutively associated with the UAV, or the UAV can be associated with a GBS at the start or the end of the mission. We define a novel *handover weight* of each edge, which is given by

$$\begin{aligned} E = &\{(U_0, G_m) : \|\boldsymbol{u}_0 - \boldsymbol{g}_m\| \leq \bar{d}_m, \ m \in \mathcal{M}\} \\ &\cup \{(G_m, G_n) : \|\boldsymbol{g}_m - \boldsymbol{g}_n\| \leq \bar{d}_m + \bar{d}_n, \ m, n \in \mathcal{M}, \ m \neq n\} \\ &\cup \{(U_{\mathrm{F}}, G_m) : \|\boldsymbol{u}_{\mathrm{F}} - \boldsymbol{g}_m\| \leq \bar{d}_m, \ m \in \mathcal{M}\}. \end{aligned} \tag{3.31}$$

Note that an edge exists between two vertices if and only if their corresponding GBSs can be potentially consecutively associated with the UAV, or the UAV can be associated with a GBS at the start or the end of the mission. We define a novel *handover weight* of each edge, which is given by

$$\begin{aligned} &W^{\mathrm{H}}(U_0, G_m) = 0, W^{\mathrm{H}}(G_m, G_n) = 1, \\ &W^{\mathrm{H}}(U_{\mathrm{F}}, G_m) = 0,\ m, n \in \mathcal{M},\ m \neq n. \end{aligned} \tag{3.32}$$

Moreover, we define a *distance weight* of each edge given by

$$\begin{aligned} &W^{\mathrm{D}}(U_0, G_m) = \|\boldsymbol{u}_0 - \boldsymbol{g}_m\|, W^{\mathrm{D}}(G_m, G_n) = \|\boldsymbol{g}_m - \boldsymbol{g}_n\|, \\ &W^{\mathrm{D}}(U_{\mathrm{F}}, G_m) = \|\boldsymbol{u}_{\mathrm{F}} - \boldsymbol{g}_m\|,\ m, n \in \mathcal{M},\ m \neq n. \end{aligned} \tag{3.33}$$

Note that any path from U_0 to U_{F} denoted by $(U_0, G_{I_0}, G_{I_1}, \cdots, G_{I_N}, U_{\mathrm{F}})$ represents a feasible GBS-UAV association sequence $\boldsymbol{I} = [I_0, \cdots, I_N]^T$, based on which the communication quality constraint can be satisfied with the proposed handover location design. The corresponding total number of handovers can be represented as $N = f^{\mathrm{H}}(\boldsymbol{I}) = W^{\mathrm{H}}(U_0, I_0) + \sum_{i=0}^{N-1} W^{\mathrm{H}}(I_{i+1}, I_i) + W^{\mathrm{H}}(I_N, U_{\mathrm{F}})$, and the corresponding mission completion time can be represented as $f^{\mathrm{T}}(\boldsymbol{I}) = (W^{\mathrm{D}}(U_0, I_0) + \sum_{i=0}^{N-1} W^{\mathrm{D}}(I_{i+1}, I_i) + W^{\mathrm{D}}(I_N, U_{\mathrm{F}}))/V_{\max}$. Thus, (P4) can be equivalently expressed as

$$(\mathrm{P5})\ \min_{\boldsymbol{I} \in \kappa}\ f^{\mathrm{H}}(\boldsymbol{I}) \tag{3.34}$$

$$\text{s.t. } f^{\mathrm{T}}(\boldsymbol{I}) \leq T_{\max}, \tag{3.35}$$

where $\kappa = \{[I_0, \cdots, I_N]^T : I_i \in \mathcal{M},\ I_i \neq I_j,\ \forall i \neq j\}$. Note that (P5) is still a non-convex optimization problem belonging to the class of *constrained shortest path problems* (or weight constrained shortest path problems), which has been shown to be NP-hard [82]. To tackle this problem, we propose an efficient

algorithm based on Lagrangian relaxation and graph theory [17]. Specifically, the Lagrangian of (P5) is given by $\mathscr{L}(\boldsymbol{I},\lambda) = f^{\mathrm{H}}(\boldsymbol{I}) + \lambda(f^{\mathrm{T}}(\boldsymbol{I}) - T_{\max})$, where $\lambda \geq 0$ denotes the dual variable associated with the constraint in (3.35). The Lagrange dual function is then given by $g(\lambda) = \min\limits_{\boldsymbol{I}} \mathscr{L}(\boldsymbol{I},\lambda) = \min\limits_{\boldsymbol{I}} f^{\mathrm{H}}(\boldsymbol{I}) + \lambda(f^{\mathrm{T}}(\boldsymbol{I}) - T_{\max})$. Consequently, the dual problem of (P5) is given by

$$\text{(P5-Dual)} \max_{\lambda \geq 0} \min_{\boldsymbol{I} \in \kappa} f^{\mathrm{H}}(\boldsymbol{I}) + \lambda(f^{\mathrm{T}}(\boldsymbol{I}) - T_{\max}). \tag{3.36}$$

(P5-Dual) is a convex optimization problem which can be solved by iteratively updating λ via the subgradient method. Due to the non-convexity of (P5), the duality gap between (P5) and (P5-Dual) is generally non-zero. To reduce this gap, we apply the K-shortest path method to obtain K best solutions for minimizing $f_{\mathrm{H}}(\boldsymbol{I}) + \lambda^{\star} f_{\mathrm{T}}(\boldsymbol{I})$ via Yen's algorithm, where $\lambda^{\star}$ is the optimal solution to (P5-Dual). Then, the final solution of $\boldsymbol{I}$ is selected as the best solution among the optimal $\boldsymbol{I}$ to (P5-Dual) and the K additional solutions. More details can be found from Appendix E of [17] and are omitted due to limited space. The worst-case complexity of this algorithm is $\mathcal{O}(M^4 \log^2 M + M^3 K)$, which is much lower than that for solving (P5) via exhaustive search, i.e., $O(M!)$ [17].

3.7. Numerical Results

In this section, we provide numerical results to evaluate the performance of our proposed handover-aware trajectory design. We set $V_{\max} = 50$ m/s, $\sigma^2 = -90$ dBm, $\beta_0 = -30$ dB, and $H = 90$ m. In Fig. 3.2, we randomly generate the locations of $M = 20$ GBSs in a 10×10 km^2 square region. We consider one large GBS indexed by 2 with transmit power 35.7 dBm and antenna height 20 m, two medium GBSs indexed by 14 and 19 with transmit power 25.6 dBm and antenna height 15 m, and 17 small GBSs with transmit power 20 dBm and antenna height 12.5 m [83].

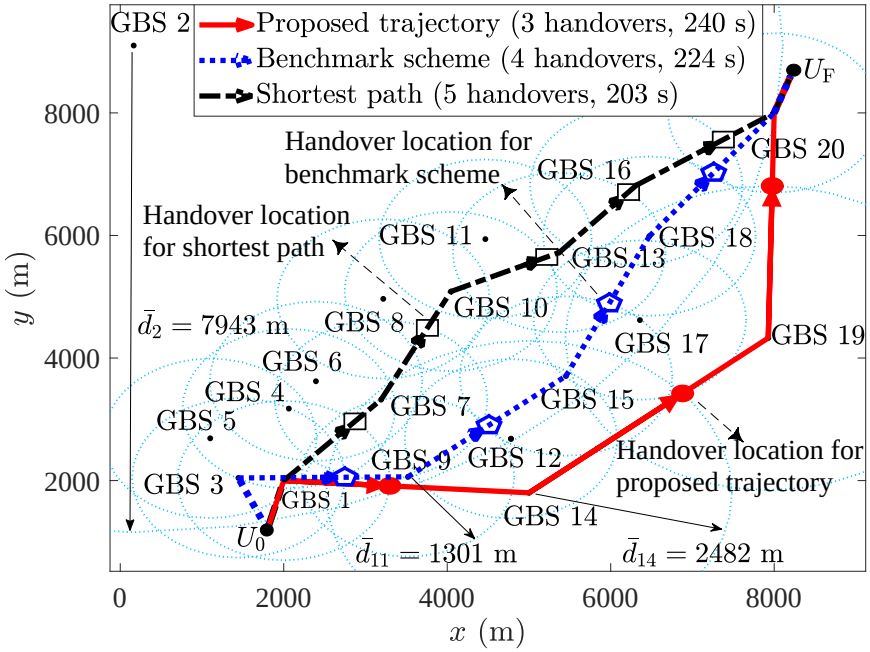

Figure 3.2: Illustration of the proposed trajectory design.

For comparison, we consider a shortest path trajectory which aims to minimize the mission completion time subject to a receive SNR constraint $\bar{\rho}$ using Method I in [15] based on a similar handover location design as in Section V-A. Moreover, we consider a benchmark scheme which aims to solve (P5) via the genetic algorithm [84]. Under a setup of $T_{\max} = 270$ s and $\bar{\rho} = 17.7$ dB, we show the trajectories via the proposed handover-aware design, the shortest path trajectory, and the benchmark scheme in Fig. 3.2. It is observed that the proposed design yields a GBS-UAV association sequence of $[1, 14, 19, 20]^T$, while the shortest path trajectory and the benchmark scheme yield sequences with more handovers, i.e., $[1, 7, 10, 13, 16, 20]^T$ and $[1, 9, 15, 18, 20]^T$, respectively. Furthermore, under $\bar{\rho} = 17.7$ dB, we show in Fig. 3.3 the number of handovers versus the mission completion time threshold $T_{\max}$ for different trajectories. It is observed that the handover performance improves as increased time is allowed for the UAV's flight, which enables higher design flexibility. In contrast, the shortest path trajectory yields a constant number of handovers which is much larger compared to the proposed design, and the benchmark scheme is also out-

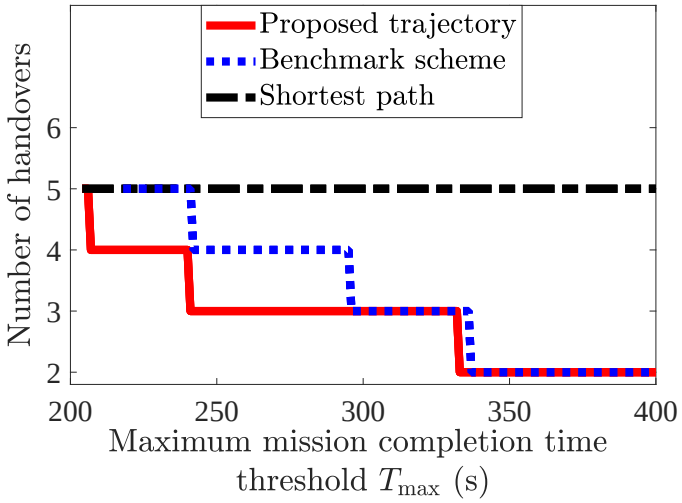

Figure 3.3: Illustration of number of handovers versus $T_{\max}$.

performed by the proposed design. Under $T_{\max} = 270$ s, we show in Fig. 3.4 the number of handovers versus the minimum SNR threshold $\bar{\rho}$. It is observed that all three designs yield larger numbers of handovers as the communication quality constraint becomes more stringent, while our proposed design still outperforms the other two schemes, thus validating its effectiveness.

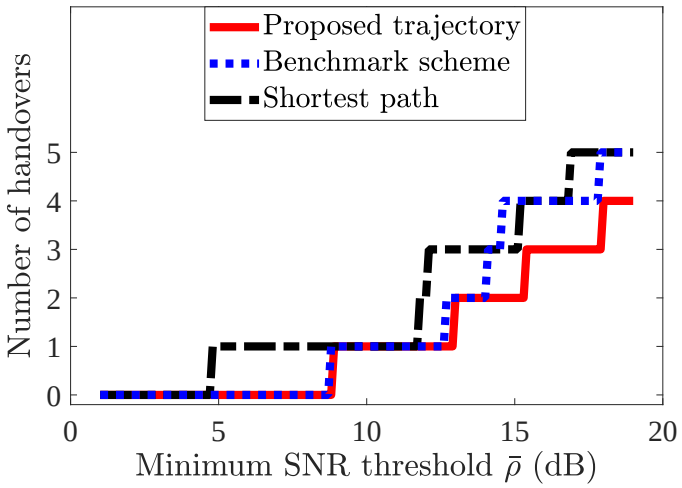

Figure 3.4: Illustration of number of handovers versus SNR threshold $\bar{\rho}$.

3.8. Chapter Summary

In this chapter, considering a cellular-connected UAV with a mission of flying between two locations, this paper studied the trajectory optimization to minimize the number of GBS handovers along the flight, subject to a communication quality constraint and a maximum mission completion time constraint. The formulated optimization problem was non-convex and involved infinite optimization variables. By exploiting the problem structure and leveraging graph theory as well as Lagrange duality, a polynomial-time algorithm was proposed to find an approximate solution. Numerical results showed that the proposed trajectory design effectively reduces the number of handovers compared with various benchmark schemes.

4. Conclusion and Future Work

4.1. Conclusion

The development of cellular-enabled UAV communication offers a promising, effective, and cost-efficient solution for various applications in future wireless communication systems. This thesis conducted in-depth studies on the trajectory optimization for cellular-connected UAVs in the face of brand new challenges in wireless communication systems. Specifically, we proposed effective high-quality solutions to address the challenges posed by new target distribution features for the target sensing mission, and we presented a handover-aware trajectory design for a cellular-connected UAV by applying various optimization methods. The findings of this study provided new insights into the design and practical implementation of cellular-connected UAV trajectories in future wireless communication systems. In the following, we summarize the main results of this thesis.

- In Chapter 2, we studied a cellular-connected UAV, where the UAV needs to complete a flight mission to sense a target. Since the exact location of the target is random and unknown, we proposed a target location distribution map to quantify the UAV's ability to sense the target. We presented three high-quality approximate solutions that have been proven to significantly enhance the UAV's sensing performance by designing the UAV's trajectory. The results provided useful guidance for the UAVs' trajectory

designs with sensing missions.

- In Chapter 3, we studied a cellular-connected UAV with a flight mission from a starting location to a final location. We took note of the handover problem in cellular networks for UAVs, and derived a handover function to characterize the relationship between the number of handovers, the UAV's flight trajectory, and the GBS-UAV association. We proposed a UAV trajectory design where the number of handovers is significantly decreased. The results provided a useful guideline for optimizing UAVs' flight trajectories to ensure high-quality communications between UAVs and GBSs.

4.2. Future Work

Based on the methods and solutions proposed in this thesis and the extension of the research results, we identify multiple promising research directions for further investigation. In the following, we list some of these interesting future research directions.

4.2.1 Trajectory Design of Cellular-connected UAVs for Target Sensing

In Chapter 2, we studied a single cellular-connected UAV, where its trajectory was designed to complete the sensing mission for one ground target. We list some future research directions and challenges as follows.

3D Trajectory Optimization: It is worthwhile extending our studies to more general 3D trajectory optimization with advanced GBS-UAV communication techniques, such as multi-GBS cooperative communication. Due to the fact that the distance between the UAV and the ground target will affect the successful sensing probability, a fundamental challenge is how to quantify UAV sensing performance when the UAV flies at different heights in complex 3D space.

Multi-Target Sensing: An important direction for future research is the exploration of multi-target sensing, where the UAV needs to simultaneously sense multiple targets, each of which may have different spatial and temporal characteristics. To this end, algorithms should be able to process the prior location information of multiple targets and design trajectories to achieve the best balance between GBS-UAV communication, the location distributions of multiple targets, and the mission completion time.

4.2.2 Handover Analysis and Handover Protocol Design for Cellular-connected UAVs

In Chapter 3, we designed a handover-aware trajectory for a cellular-connected UAV to complete its flight mission. There are several aspects of handover that require deeper analysis and more refined protocol development to improve reliability and efficiency.

Comprehensive Handover Analysis: It is worth noting that a more detailed analysis of the handover process should be considered for cellular-enabled UAV communication, including factors such as handover failure probability, the probability of the ping-pong effect, and handover duration. Detailed studies on handover duration and its impact on service quality in UAV communication will also be critical.

Actual Ground-to-Air Channel: The actual shape of the coverage area, influenced by factors such as antenna tilt and environmental variables (e.g., obstacles), is rarely a perfect circle. Future work should consider these real-world complexities in the ground-to-air channel to refine trajectory optimization algorithms, thus enhancing communication quality between UAVs and GBSs.

4.2.3 Trajectories Design for Multi-UAV

Employing multi-UAV or a UAV swarm can not only significantly reduce the time required for sensing but also enhance mission performance. However, this approach introduces new challenges that must be addressed.

Dynamic Mission Allocation: Research should focus on developing dynamic mission allocation frameworks that can respond in real-time to changing conditions and mission demands, optimizing resource use across multiple UAVs. The trajectories of multiple UAVs should be jointly optimized with the consideration of mission allocation to maximize mission performance.

Complex Communication Networks: Future studies should focus on deploying advanced network architectures, possibly utilizing emerging technologies like 6G networks, to support high-capacity communications for multiple UAVs. Meanwhile, effective communication interference management technology or beamforming technology should also be proposed for enhancing multi-UAV communications.

Collision Avoidance Systems: As the density of UAV operations increases, so does the risk of in-air collisions. Future work must develop more advanced collision avoidance systems that integrate real-time sensory data and predictive analytics to ensure safe operations.

Bibliography

[1] G. Geraci, A. Garcia-Rodriguez, M. M. Azari, A. Lozano, M. Mezzavilla, S. Chatzinotas, Y. Chen, S. Rangan, and M. D. Renzo, "What will the future of UAV cellular communications be? a flight from 5G to 6G," *IEEE Commun. Surv. Tut.*, vol. 24, no. 3, pp. 1304–1335, second quarter 2022.

[2] Z. Wei, M. Zhu, N. Zhang, L. Wang, Y. Zou, Z. Meng, H. Wu, and Z. Feng, "UAV-assisted data collection for internet of things: A survey," *IEEE Internet Things J.*, vol. 9, no. 17, pp. 15 460–15 483, Sep. 2022.

[3] H. Wang, H. Zhao, J. Zhang, D. Ma, J. Li, and J. Wei, "Survey on unmanned aerial vehicle networks: A cyber physical system perspective," *IEEE Commun. Surv. Tut.*, vol. 22, no. 2, pp. 1027–1070, second quarter 2020.

[4] Y. Zeng, Q. Wu, and R. Zhang, "Accessing from the sky: A tutorial on UAV communications for 5G and beyond," *Proc. IEEE*, vol. 107, no. 12, pp. 2327–2375, Dec. 2019.

[5] Y. Bai, H. Zhao, X. Zhang, Z. Chang, R. Jäntti, and K. Yang, "Toward autonomous multi-UAV wireless network: A survey of reinforcement learning-based approaches," *IEEE Commun. Surv. Tut.*, vol. 25, no. 4, pp. 3038–3067, fourth quarter 2023.

[6] H. Kurunathan, H. Huang, K. Li, W. Ni, and E. Hossain, "Machine learning-aided operations and communications of unmanned aerial vehi-

cles: A contemporary survey," *IEEE Commun. Surv. Tut.*, vol. 26, no. 1, pp. 496–533, first quarter 2024.

[7] W. S. R. Souza, A. J. Hart, B. J. B. Fonseca, M. Tahernezhadi, and L. E. Christensen, "A framework to survey a region for gas leaks using an unmanned aerial vehicle," *IEEE Access*, vol. 12, pp. 1386–1407, Dec. 2023.

[8] S. K. Sonkar, P. Kumar, R. C. George, D. Philip, and A. K. Ghosh, "Detection and estimation of natural gas leakage using UAV by machine learning algorithms," *IEEE Sensors J.*, vol. 22, no. 8, pp. 8041–8049, Mar. 2022.

[9] N. Shirakura, T. Kiyokawa, H. Kumamoto, J. Takamatsu, and T. Ogasawara, "Collection of marine debris by jointly using UAV-UUV with GUI for simple operation," *IEEE Access*, vol. 9, pp. 67 432–67 443, Apr. 2021.

[10] R. Akter, M. Golam, V.-S. Doan, J.-M. Lee, and D.-S. Kim, "IoMT-Net: Blockchain-integrated unauthorized UAV localization using lightweight convolution neural network for internet of military things," *IEEE Internet Things J.*, vol. 10, no. 8, pp. 6634–6651, Apr. 2023.

[11] W. Alexan, L. Aly, Y. Korayem, M. Gabr, D. El-Damak, A. Fathy, and H. A. A. Mansour, "Secure communication of military reconnaissance images over UAV-assisted relay networks," *IEEE Access*, vol. 12, pp. 78 589–78 610, May 2024.

[12] P. K. Reddy Maddikunta, S. Hakak, M. Alazab, S. Bhattacharya, T. R. Gadekallu, W. Z. Khan, and Q.-V. Pham, "Unmanned aerial vehicles in smart agriculture: Applications, requirements, and challenges," *IEEE Sensors J.*, vol. 21, no. 16, pp. 17 608–17 619, Aug. 2021.

[13] S. K. Phang, T. H. A. Chiang, A. Happonen, and M. M. L. Chang, "From satellite to UAV-based remote sensing: A review on precision agriculture," *IEEE Access*, vol. 11, pp. 127 057–127 076, Dec. 2023.

[14] A. Masaracchia, L. D. Nguyen, T. Q. Duong, C. Yin, O. A. Dobre, and E. Garcia-Palacios, "Energy-efficient and throughput fair resource allocation for TS-NOMA UAV-assisted communications," *IEEE Trans. Commun.*, vol. 68, no. 11, pp. 7156–7169, Nov. 2020.

[15] S. Zhang, Y. Zeng, and R. Zhang, "Cellular-enabled UAV communication: A connectivity-constrained trajectory optimization perspective," *IEEE Trans. Commun.*, vol. 67, no. 3, pp. 2580–2604, Mar. 2019.

[16] Y. Zeng, J. Lyu, and R. Zhang, "Cellular-connected UAV: Potential, challenges, and promising technologies," *IEEE Wireless Commun.*, vol. 26, no. 1, pp. 120–127, Sep. 2019.

[17] S. Zhang and R. Zhang, "Trajectory optimization for cellular-connected UAV under outage duration constraint," *J. Commun. Inf. Netw.*, vol. 4, no. 4, pp. 55–71, Dec. 2019.

[18] N. Senadhira, S. Durrani, X. Zhou, N. Yang, and M. Ding, "Uplink NOMA for cellular-connected UAV: Impact of UAV trajectories and altitude," *IEEE Trans. Commun.*, vol. 68, no. 8, pp. 5242–5258, Aug. 2020.

[19] S. Zhang and R. Zhang, "Radio map-based 3D path planning for cellular-connected UAV," *IEEE Trans. Wireless Commun.*, vol. 20, no. 3, pp. 1975–1989, Mar. 2021.

[20] X. Guo, S. Zhang, and L. Liu, "Trajectory optimization of cellular-connected UAV for information collection and transmission," in *Proc. IEEE Global Commun. Conf. (GLOBECOM)*, Dec. 2022, pp. 5977–5982.

[21] X. Pang, W. Mei, N. Zhao, and R. Zhang, "Intelligent reflecting surface assisted interference mitigation for cellular-connected UAV," *IEEE Wireless Commun. Lett.*, vol. 11, no. 8, pp. 1708–1712, Aug. 2022.

[22] C. Zhan and Y. Zeng, "Energy minimization for cellular-connected UAV: From optimization to deep reinforcement learning," *IEEE Tran. Wireless Commun.*, vol. 21, no. 7, pp. 5541–5555, Jul. 2022.

[23] B. Yang, T. Taleb, and G. Chen, "On sum rate maximization study for cellular-connected UAV swarm communications," in *Proc. IEEE Int. Conf. Commun. (ICC)*, Aug. 2021, pp. 1–6.

[24] H. Zhao, Q. Hao, H. Huang, G. Gui, T. Ohtsuki, H. Sari, and F. Adachi, "Online trajectory optimization for energy-efficient cellular-connected UAVs with map reconstruction," *IEEE Trans. Veh. Technol.*, vol. 73, no. 3, pp. 3445–3456, Mar. 2024.

[25] P. Li, L. Xie, J. Yao, and J. Xu, "Cellular-connected UAV with adaptive Air-to-Ground interference cancellation and trajectory optimization," *IEEE Commun. Lett.*, vol. 26, no. 6, pp. 1368–1372, Jun. 2022.

[26] Q. Hao, H. Zhao, H. Huang, G. Gui, T. Ohtsuki, and F. Adachi, "Deep reinforcement learning aided online trajectory optimization of cellular-connected UAVs with offline map reconstruction," in *Proc. IEEE Veh. Technol. Conf. (VTC) Spring*, Jun. 2023, pp. 1–5.

[27] C. Zhan and Y. Zeng, "Energy-efficient data uploading for cellular-connected UAV systems," *IEEE Trans. Wireless Commun.*, vol. 19, no. 11, pp. 7279–7292, Nov. 2020.

[28] Y. Zeng and X. Xu, "Path design for cellular-connected UAV with reinforcement learning," in *Proc. IEEE Global Commun. Conf. (GLOBECOM)*, Feb. 2020, pp. 1–6.

[29] Y. Qin, M. A. Kishk, and M.-S. Alouini, "Coverage analysis and trajectory optimization for aerial users with dedicated cellular infrastructure," *IEEE Trans. Wireless Commun.*, vol. 23, no. 4, pp. 3042–3056, Apr. 2024.

[30] B. Liu and M. Peng, "Online offloading for energy-efficient and delay-aware MEC systems with cellular-connected UAVs," *IEEE Internet Things J.*, vol. 11, no. 12, pp. 22 321–22 336, Jun. 2024.

[31] B. Khamidehi and E. S. Sousa, "Federated learning for cellular-connected UAVs: Radio mapping and path planning," in *Proc. IEEE Global Commun. Conf. (GLOBECOM)*, Jan. 2021, pp. 1–6.

[32] Y. Li, A. H. Aghvami, and D. Dong, "Path planning for cellular-connected UAV: A DRL solution with quantum-inspired experience replay," *IEEE Trans. Wireless Commun.*, vol. 21, no. 10, pp. 7897–7912, Oct. 2022.

[33] K. Meng, Q. Wu, J. Xu, W. Chen, Z. Feng, R. Schober, and A. L. Swindlehurst, "UAV-enabled integrated sensing and communication: Opportunities and challenges," *IEEE Wireless Commun.*, vol. 31, no. 2, pp. 97–104, Apr. 2024.

[34] Z. Huang, C. Chen, and M. Pan, "Multiobjective UAV path planning for emergency information collection and transmission," *IEEE Internet Things J.*, vol. 7, no. 8, pp. 6993–7009, Aug. 2020.

[35] J. Wang, H. Zhang, X. Zhou, and D. Yuan, "UAV-assisted wireless networks: Mobility and service oriented power allocation and trajectory design," *IEEE Trans. Veh. Technol.*, early access, doi: 10.1109/TVT.2024.3430370.

[36] W. Liu, H. Wang, X. Zhang, H. Xing, J. Ren, Y. Shen, and S. Cui, "Joint trajectory design and resource allocation in UAV-enabled heterogeneous MEC systems," *IEEE Internet Things J.*, early access, doi: 10.1109/JIOT.2024.3418568.

[37] Y. Wang, M. Chen, C. Pan, K. Wang, and Y. Pan, "Joint optimization of UAV trajectory and sensor uploading powers for UAV-assisted data collec-

tion in wireless sensor networks," *IEEE Internet Things J.*, vol. 9, no. 13, pp. 11 214–11 226, Jul. 2022.

[38] S. Zhang, H. Zhang, B. Di, and L. Song, "Joint trajectory and power optimization for UAV sensing over cellular networks," *IEEE Commun. Lett.*, vol. 22, no. 11, pp. 2382–2385, Nov. 2018.

[39] Y. Yu, X. Liu, Z. Liu, and T. S. Durrani, "Joint trajectory and resource optimization for RIS assisted UAV cognitive radio," *IEEE Trans. Veh. Technol.*, vol. 72, no. 10, pp. 13 643–13 648, Oct. 2023.

[40] X. Jiang, Z. Wu, Z. Yin, W. Yang, and Z. Yang, "Trajectory and communication design for UAV-relayed wireless networks," *IEEE Wireless Commun. Lett.*, vol. 8, no. 6, pp. 1600–1603, Dec. 2019.

[41] S. Zhang, J. Yang, H. Zhang, and L. Song, "Dual trajectory optimization for a cooperative internet of UAVs," *IEEE Commun. Lett.*, vol. 23, no. 6, pp. 1093–1096, Jun. 2019.

[42] Z. Liu, X. Liu, Y. Liu, V. C. M. Leung, and T. S. Durrani, "UAV assisted integrated sensing and communications for internet of things: 3D trajectory optimization and resource allocation," *IEEE Trans. Wireless Commun.*, vol. 23, no. 8, pp. 8654–8667, Aug. 2024.

[43] Z. Lyu, G. Zhu, and J. Xu, "Joint maneuver and beamforming design for UAV-enabled integrated sensing and communication," *IEEE Trans. Wireless Commun.*, vol. 22, no. 4, pp. 2424–2440, Apr. 2022.

[44] C. Deng, X. Fang, and X. Wang, "Beamforming design and trajectory optimization for UAV-Empowered adaptable integrated sensing and communication," *IEEE Trans. Wireless Commun.*, vol. 22, no. 11, pp. 8512–8526, Apr. 2023.

[45] H. V. Nguyen, H. Rezatofighi, B.-N. Vo, and D. C. Ranasinghe, "Online UAV path planning for joint detection and tracking of multiple radio-tagged objects," *IEEE Trans. Signal Process.*, vol. 67, no. 20, pp. 5365–5379, Sep. 2019.

[46] Y. Yu, H. Wang, S. Liu, L. Guo, P. L. Yeoh, B. Vucetic, and Y. Li, "Distributed multi-agent target tracking: A nash-combined adaptive differential evolution method for UAV systems," *IEEE Trans. Veh. Technol.*, vol. 70, no. 8, pp. 8122–8133, Jun. 2021.

[47] K. Tanaka, M. Tanaka, Y. Takahashi, A. Iwase, and H. O. Wang, "3-D flight path tracking control for unmanned aerial vehicles under wind environments," *IEEE Trans. Veh. Technol.*, vol. 68, no. 12, pp. 11 621–11 634, Oct. 2019.

[48] J. Mu, R. Zhang, Y. Cui, N. Gao, and X. Jing, "UAV meets integrated sensing and communication: Challenges and future directions," *IEEE Commun. Magazine*, vol. 61, no. 5, pp. 62–67, Jan. 2023.

[49] C. Diaz-Vilor, M. A. Almasi, A. M. Abdelhady, A. Celik, A. M. Eltawil, and H. Jafarkhani, "Sensing and communication in UAV cellular networks: Design and optimization," *IEEE Trans. Wireless Commun.*, vol. 23, no. 6, pp. 5456–5472, Oct. 2023.

[50] D. Liu, Y. Gao, S. Hu, W. Ni, and X. Wang, "Trajectory design for integrated sensing and communication enabled by cellular-connected UAV," *IEEE Wireless Commun. Lett.*, vol. 13, no. 7, pp. 1973–1977, May 2024.

[51] S. Hu, X. Yuan, W. Ni, and X. Wang, "Trajectory planning of cellular-connected UAV for communication-assisted radar sensing," *IEEE Trans. Commun.*, vol. 70, no. 9, pp. 6385–6396, Sep. 2022.

[52] Y. Liu, S. Liu, X. Liu, Z. Liu, and T. S. Durrani, "Sensing fairness-based energy efficiency optimization for UAV enabled integrated sensing and communication," *IEEE Wireless Commun. Lett.*, vol. 12, no. 10, pp. 1702–1706, Oct. 2023.

[53] X. Zhang, M. Peng, and C. Liu, "Sensing-assisted beamforming and trajectory design for UAV-enabled networks," *IEEE Trans. Veh. Technol.*, vol. 73, no. 3, pp. 3804–3819, Mar. 2024.

[54] K. Meng, Q. Wu, S. Ma, W. Chen, K. Wang, and J. Li, "Throughput maximization for UAV-enabled integrated periodic sensing and communication," *IEEE Trans. Wireless Commun.*, vol. 22, no. 1, pp. 671–687, Aug. 2022.

[55] S. Zhang, H. Zhang, Z. Han, H. V. Poor, and L. Song, "Age of information in a cellular internet of UAVs: Sensing and communication trade-off design," *IEEE Trans. Wireless Commun.*, vol. 19, no. 10, pp. 6578–6592, Jun. 2020.

[56] C. Xu and S. Zhang, "MIMO radar transmit signal optimization for target localization exploiting prior information," in *Proc. IEEE Int. Symp. Inf. Theory (ISIT)*, Jun. 2023, pp. 310–315.

[57] K. Hou and S. Zhang, "Secure integrated sensing and communication exploiting target location distribution," in *Proc. IEEE Global Commun. Conf. (GLOBECOM)*, Dec. 2023, pp. 4933–4938.

[58] C. Xu and S. Zhang, "MIMO integrated sensing and communication exploiting prior information," *IEEE J. Sel. Areas Commun.*, early access, doi: 10.1109/JSAC.2024.3413972.

[59] K. Hou and S. Zhang, "Optimal beamforming for secure integrated sensing and communication exploiting target location distribution," [Online]. Available: https://arxiv.org/abs/2312.13797.

[60] U. Challita, W. Saad, and C. Bettstetter, "Interference management for cellular-connected UAVs: A deep reinforcement learning approach," *IEEE Trans. Wireless Commun.*, vol. 18, no. 4, pp. 2125–2140, Apr. 2019.

[61] H. Wei and H. Zhang, "Time-varying boundary modeling and handover analysis of UAV-assisted networks with fading," *IEEE Trans. Wireless Commun.*, vol. 23, no. 7, pp. 7552–7565, Dec. 2023.

[62] A. Colpaert, E. Vinogradov, and S. Pollin, "3D beamforming and handover analysis for UAV networks," in *Proc. IEEE Globecom Workshops (GC Wkshps)*, Mar. 2021, pp. 1–6.

[63] H. Wei and H. Zhang, "Equivalent modeling and analysis of handover process in K-Tier UAV networks," *IEEE Trans. Wireless Commun.*, vol. 22, no. 12, pp. 9658–9671, May 2023.

[64] J. Zhao, C. Zhang, W. Zheng, and Z. Lu, "Seamless time sensitive handover scheme based on CoMP-JT for 5G-enabled autonomous driving," in *Proc. IEEE Int. Conf. Commun. Workshops (ICC Wkshps)*, Sep. 2022, pp. 1–6.

[65] Z. Liu, E. Zhou, J. Cui, Z. Dong, and P. Fan, "A double-beam soft handover scheme and its performance analysis for mmWave UAV communications in windy scenarios," *IEEE Trans. Veh. Technol.*, vol. 72, no. 1, pp. 893–906, Dec. 2023.

[66] N. K. Panigrahy and S. C. Ghosh, "Analyzing the effect of soft handover on handover performance evaluation metrics under load condition," *IEEE Trans. Veh. Technol.*, vol. 67, no. 4, pp. 3612–3624, Apr. 2018.

[67] H. Khalid, S. J. Hashim, F. Hashim, S. M. Syed Ahamed, M. A. Chaudhary, H. H. M. Altarturi, and M. Saadoon, "HOOPOE: High performance and efficient anonymous handover authentication protocol for flying out of zone

UAVs," *IEEE Trans. Veh. Technol.*, vol. 72, no. 8, pp. 10 906–10 920, Aug. 2023.

[68] Y. Aydin, G. K. Kurt, E. Ozdemir, and H. Yanikomeroglu, "Group handover for drone base stations," *IEEE Internet Things J.*, vol. 8, no. 18, pp. 13 876–13 887, Sep. 2021.

[69] D. Kwon, S. Son, Y. Park, H. Kim, Y. Park, S. Lee, and Y. Jeon, "Design of secure handover authentication scheme for urban air mobility environments," *IEEE Access*, vol. 10, pp. 42 529–42 541, Apr. 2022.

[70] S. Horsmanheimo, L. Tuomimäki, V. Semkin, S. Mehnert, T. Chen, M. Ojennus, and L. Nykänen, "5G communication QoS measurements for smart city UAV services," in *Proc. 16th Eur. Conf. Antennas Propagat. (EuCAP)*, Apr. 2022, pp. 1–5.

[71] M. Gharib, S. Nandadapu, and F. Afghah, "An exhaustive study of using commercial LTE network for UAV communication in rural areas," in *Proc. IEEE Int. Conf. Commun. Workshops (ICC Wkshps)*, Jul. 2021, pp. 1–6.

[72] M. Banagar, V. V. Chetlur, and H. S. Dhillon, "Handover probability in drone cellular networks," *IEEE Wireless Commun. Lett.*, vol. 9, no. 7, pp. 933–937, Jul. 2020.

[73] Y. Guo and H. Zhang, "3D boundary modeling and handover analysis of aerial users in heterogeneous networks," *IEEE Trans. Veh. Technol.*, vol. 72, no. 10, pp. 13 523–13 529, May 2023.

[74] V. Sharma, F. Song, I. You, and H.-C. Chao, "Efficient management and fast handovers in software defined wireless networks using UAVs," *IEEE Netw.*, vol. 31, no. 6, pp. 78–85, Dec. 2017.

[75] Z. Liu, E. Zhou, J. Cui, Z. Dong, and P. Fan, "A double-beam soft handover scheme and its performance analysis for mmWave UAV communications in windy scenarios," *IEEE Trans. Veh. Technol.*, vol. 72, no. 1, pp. 893–906, Sep. 2022.

[76] W. Liu and J. Chen, "UAV-aided radio map construction exploiting environment semantics," *IEEE Trans. Wireless Commun.*, vol. 22, no. 9, pp. 6341–6355, Feb. 2023.

[77] C. He, Y. Dong, and Z. J. Wang, "Radio map assisted multi-UAV target searching," *IEEE Trans. Wireless Commun.*, vol. 22, no. 7, pp. 4698–4711, Dec. 2022.

[78] S. Bi, J. Lyu, Z. Ding, and R. Zhang, "Engineering radio maps for wireless resource management," *IEEE Wireless Commun.*, vol. 26, no. 2, pp. 133–141, Feb, 2019.

[79] K. Meng, Q. Wu, S. Ma, W. Chen, and T. Q. S. Quek, "UAV trajectory and beamforming optimization for integrated periodic sensing and communication," *IEEE Wireless Commun. Lett.*, vol. 11, no. 6, pp. 1211–1215, Jun. 2022.

[80] G. Y. Handler and I. Zang, "A dual algorithm for the constrained shortest path problem," *Networks*, vol. 10, no. 4, 1980.

[81] D. B. West, *Introduction to Graph Theory.* Prentice Hall, 2001.

[82] M. R. Gary and D. S. Johnson, "Computers and intractability: Guide to the theory of NP-completeness," New York: W. H. Freeman and Company, 1979.

[83] 3GPP, "Enhanced LTE support for aerial vehicles," V15.0.0, 2017.

[84] M. Mitchell, *An Introduction to Genetic Algorithms.* MIT press, 1998.